SPE 159380

A Fully Coupled Model of Nonisothermal Multiphase Flow, Solute Transport and Reactive Chemistry in Porous Media

Ronglei Zhang, Xiaolong Yin, Yu-Shu Wu, Philip H. Winterfeld, Colorado School of Mines

This paper was prepared for presentation at the SPE Annual Technical Conference and Exhibition held in San Antonio, Texas, USA, 8-10 October 2012.

Abstract

Over the past decades, geochemical reaction has been identified through experiments in different processes, e.g. the CO_2 EOR process, the CO_2 sequestration, the enhanced geothermal system. Research has gradually led to the recognition that chemical reactions between injected fluid and mineral rock have significant impacts on fluid dynamics and rock properties in these processes. However, for the majority of the reactive transport simulators, the sequential calculation processes of fluid flow, solute transport, and reactive geochemistry result in numerical instability and computation efficiency problems. In this paper, we present a fully coupled computational framework to simulate reactive solute transport in porous media for mixtures having an arbitrary number of phases. The framework is designed to keep a unified computational structure for different physical processes. This fully coupled simulator focuses on: (1) the fluid flow, solute transport, and chemical reactions within a three-phase mixture, (2) physically and chemically heterogeneous porous and fractured rocks, (3) the non-isothermal effect on fluid properties and reaction processes, and (4) the kinetics of fluid-rock and gas-rock interactions. In addition, a system of partial differential equations is formed to represent the physical and chemical processes of reactive solute transport. A flexible approach of integral finite difference is employed to to obtain the residuals of the equation system. Jacobin matrix for Newton-Raphson iteration is generated by numerical calculation, which helps the future parallelization of the fully coupled simulator. Finally, the fully coupled model is validated using the TOUGHREACT simulator. Examples with practical interests will be discussed, including CO_2 flooding in a reservoir, supercritical CO_2 injection into a saline aquifer, and cold water injection into a natural geothermal reservoir. This type of simulation is very important for modeling of physical processes, especially for CO_2 EOR and storage, and geothermal resources development.

Inroduction

Reactive fluid flow and geochemical species transport that occur in subsurface reservoirs have been of increasing interest to researchers in the subjects of CO_2 geological sequestration, CO_2 EOR process, enhanced geothermal system, or even waterflooding and other EOR processes. The chemical reaction path has been observed in these processes when subjected to fluid injection in the subsurface reservoir. The nonisothermal reactive solute transport phenomena involed in these processes are thermal-hydrological-chemical (THC) processes. However, the reaction paths may be slightly different due to the different fluid flow mechanisms related to these processes.

CO_2 geological sequestration and CO_2 EOR are two effective solutions to store CO_2 from burning fossil fuels in geological formations and petroleum reservoirs. Saline aquifers and petroleum reservoirs have the largest capacity among the many options for long-term geological sequestration. They are large underground formations saturated with brine water or hydrcarbons, and are often rich in dissolved minerals. CO_2 is injected into these formations as a supercritical fluid with a liquid-like density and a gas-like viscosity. It is believed that geochemical reaction between CO_2 and rock minerals in the aqueous–based system dominates the long-term fate of CO_2 sequestrated in geological formations. Two types of geochemical reactions between CO_2 and rock minerals have been identified by experiments, i.e. reactions between dissolved CO_2 and rock minerals, and reactions between supercritical CO_2 and rock minerals. The chemical mechanism between dissolved CO_2 and rock mineral has been well understood. The acid H_2CO_3 is formed by the dissolution of CO_2 in an aqueous solution, and it dissociates in the brine to release H^+. The carbonate minerals are dissolved into the aqueous phase under this weak acid

environment, which will rapidly buffer the pH and render the aqueous solution less acid. Also, the alternation of feldspars and clay minerals can precipitate carbonate mineral to trap CO_2 in solid phase permanently. Majority of these geochemical reactions in aqueous phase has been identified in many experiments (e.g., Credoz et al., 2009; Kaszuba et al., 2003; Wigand et al., 2008). However, the reaction between supercritical CO_2 (or anhydrous CO_2) and rock minerals is less studied, some previous experiments (Jacquemet et al., 2008; Regnault et al., 2005, 2009) indicated that supercritical CO_2 led to the alternation of portlandite under kinetic condition. These reactions may affect the wellbore integrity and aquifer matrix rock injectivity. Further investigation of the significance of these reactions is needed. On the other hand, numerical simulations (Audigane et al., 2007; White et al., 2001, 2005; Xu et al., 2004, 2006, 2010) have been carried out to model the trapping mechanism of geochemical reactions in aqueous phase, but few studies considered the influence of geochemical reactions between supercritical CO_2 and rock minerals.

Unlike the process of CO_2 sequestration, geochemical reactions in an EGS reservoir only take place in aqueous phase, which is a non-isothermal system. Stimulation fluids used in EGS development typically are aqueous-based. Subsequently, aqueous-based reservoir stimulation is likely to trigger dissolution and precipitation of rock minerals. The typical geochemical reactions in EGS reservoirs include the dissolution of carbonate minerals and silica minerals, releasing CO_3^{2-}, HCO_3^-, $CO_2(aq)$, H^+, Ca^{2+}, Mg^{2+}, $SiO_2(aq)$, etc. These reactions are under kinetic condition and controlled by related kinetic rate constants, depending temperature. These kinetic reactions may be accelerated in an EGS reservoir at high temperature. Accordingly, the dissolved aqueous species in the complex electron environment can react with each other to precipitate ontoother minerals, which may lead to large impact on the permeability of the fracture network and on the rate at which fluids can be circulated to bring usable heat to the land surface. In order to assist the development of geothermal energy, chemical interactions between rocks and fluids should be evaluated and predicted.

It is a challenging issue to model the THC processes mathematically, because of the complexity of multiphase fluid flow, water-gas-rock interaction, and the strong non-linearities in the mass and energy consservation equations. There are two major methods widely used to solve the fluild flow, solute transport, and geochemical reactions together, i.e. direct substitution approach and sequential iteration approach. Among them, the sequential iteration approach solves the transport and the reaction equations separately in a sequential manner with an iterative procedure (Cederberg et al., 1985; Nienhuis et al., 1991; Yeh and Tripathi, 1991; Engesgaard and Kipp, 1992; Simunek and Suares, 1994; Walter et al., 1994; Zysset et al., 1994; Xu, 1996; Wei, 2012). Furthermore, a modified sequential noniterative approach was proposed to solve solute transport and chemistry only once without iteration (Liu and Narasimhan, 1989; Ague and Brimhall, 1989; Appelo, 1994). By means of the sequential iteration approach, a set of geochemical codes such as EQ3/6 (Wolery, 1992), PHREEQE (Parkhurst et al., 1980), PHREEQC V2.0 (Parkhurst and Appelo, 1999), GEOCHEMIST'S WORKBENCH (Bethk, 2002), TOUGHREACT (Xu and Puress, 1998), and UTCHEM (Delshad et al. 1996, Fathi Najafabadi et al., 2009) are designed to couple the fluid flow, solute transport, and geochemical reaction sequentially. Among them, EQ3/6, PHREEQC, GEOCHEMIST'S WORKBENCH are for batch reaction systems or 1D geochemistry transport problems, and keep track of the full chemical database during the entire simulation. This may be not efficient or impractical for simulating field-scale multidimensional reactive transport problems. TOUGHREACT and UTCHEM are developed to solve the multi-dimensional and multi-phase fluid flow, solute transport, and chemical reactions in groundwater and petroleum systems, respectively. UTCHEM does not consider the kinetic reactions. Even though the sequential iteration approach and its modified version are widely used, it has some concern with this approach's numerical stability and accuracy (Yeh and Tripathi, 1989). The second method, direct substitution approach, substitutes the geochemical reaction into the fluid flow equations directly, forming a fully coupled reactive solute transport model. This approach solves the fluid flow, solute transport, and geochemical reactions simultaneously with a high accuracy. Even though it might consume more computer resources than the sequential iteration approach, the parallel computing could solve this problem easily.

In this paper, we take a closer look at the original code structure of TOUGHREACT simulator (Xu and Puress, 1998), as a representative of the simulators employing the sequential iteration approach, including the numerical method, the solution sequence, and the code architecture. Secondly, based on the structure of TOUGHREACT simulator, the framework of a fully coupled reactive solute transport model is proposed to keep a unified computational structure for different physical processes. Furthermore, we present a fully coupled modeling approach for non-isothermal multiphase fluid flow and geochemical transport, and the mathematical equations for the model are decribed in detail. This fully coupled simulator has the following features: (1) the fluid flow, solute transport, and chemical reactions within a three-phase mixture, (2) physically and chemically heterogeneous porous and fractured rocks, (3) the non-isothermal effect on fluid properties and reaction processes, and (4) the kinetics of fluid-rock and gas-rock interactions. This code provides a detailed description of rock-fluid interactions during multiphase, nonisothermal flow, and transport in porous media. Finally, two geochemical reaction systems subjected to the environment of supercritical CO_2 are simulated by the full coupled model. The first one is a batch geochemical system, considering the chemical interaction of gas-liquid-mineral (CO_2 (g)-H_2O-NaCl-$CaCO_3$) in the quilibrium state, and the simulation result is validated by the TOUGHREACT simulator. The second one is a bactch system with complex geochemistry, which considering the chemical equilibrium and kinetics simultaneously. The geochemical reactions and the

rock mineral compositions are representative in the potential geological formations for CO_2 sequestration CO_2 EOR, water flooding IOR and enhanced geothermal system.

1. The code architechure of the fully coupled reactive solute transport model

Code Structure of TOUGHREACT Simulator

The code structure of TOUGHREACT is taken as a basic reference to propose the structure of the fully coupled reactive solute transport model. Fig. 1 shows the flow chart for solving the coupled non-isothermal multiphase fluid flow, solute transport, and reactive geochemistry in TOUGHREACT simulator. There are three main parts: the fluid flow and heat transfer, the solute transport of aqueous and gaseous species, and the geochemical reaction. These three parts are shown in the red boxes of Fig. 1. The multiphase fluid and heat flow equations are solved first, and the resulting fluid velocity is substituted into the solute transport equations, which are treated in terms of total dissolved concentrations of primary chemical species for the aqueous solute, and gaseous partial pressure for gas transport. The resulting concentrations and partial pressures from the transport calculation are substituted into the chemical reaction submodel, which is solved on a grid block basis. The change of gaseous partial pressure due to dissolution does not feed back to the overall fluid flow of chemical species, and there is on feedback of mass or energy between fluid flow and reactive solute transport (Xu et al., 2004). The transport and reaction equations are solved iteratively until convergence. The convergences of fluid flow and reactive solute transport may not be achieved in the same time step (Xu, et al., 2006). During a transport time step Δt_v, depending on the convergence of the reaction equations, multiple time steps with $\Sigma\Delta t_r = \Delta t_v$, can be used. The Δt_r may be different from grid block to grid block depending on the convergence behavior of the local chemical reaction system.

The solution method of TOUGHREACT simulator is as follows: the equation system of fluid and heat flow equations is a set of non-linear algebraic equations for the thermodynamic state variables in all grid blocks as unknowns. These are solved by Newton-Raphson iteration in the TOUGHREACT simulator (Xu et al., 2004). The matrix coefficients are calculated by numerical derivatives related to the primary unknown variables. The set of coupled linear equations arising at each iteration step is solved iteratively by means of preconditioned conjugate gradient methods (Moridis and Pruess, 1998). The conjugate gradient solver is 'T2CG2' in TOUGHREACT code. In addition, a sequential non-iterative approach is used to solve the transport and reaction equations, the solute transport equations and chemical reaction equations are considered as two relatively independent subsystems. They are solved separately in a sequential manner following an iterative procedure. For the solute transport, the transport of gaseous species and aqueous species are solved separately, the conjugate gradient solver 'T2CG2' is used twice to solve the solute transport. Finally, the geochemical reaction system is still a set of non-linear algebraic equations and solve by Newton-Raphson iteration. The matrix coefficients are calculated by analytical derivatives related to the primary unknown variables, and solved by the LU solver ('ludcmp' and 'lubksb'). The flow chart of solving procedure in TOUGHREACT simulator is shown in Fig. 2.

Code Structure for the Fully Coupled Model

Fig. 3 shows the new flow chart for solving coupled processes of non-isothermal multiphase fluid flow, solute transport, and reactive geochemistry in the fully coupled simulator. It solves the fluid flow, solute transport, and geochemical reactions simultaneously. The development of this fully coupled model is based on the TOUGH family code (Puress, 1990) and TOUGHREACT code (Xu and Puress, 1998). The mass balance equation for each primary component or chemical species is constructed. These equations are highly non-linear algebraic equations when taking the geochemical reaction into account. They are solved by the Newton-Raphson iteration method, and the Jacobin matrix coefficients are calculated by the numerical approach. The **multi** module in TOUGH family code is rewritten due to the increased numer of mass balance equations and chemical constraints equations. The number of equations in the equation system may be three to six times larger than that of the original equation system in the fluid flow part. The conjugate gradient solver will be used once to solve the whole fluid flow, solute transport, and chemical reactions. In addition, for phase behavior and fluid property calculation, the EOS module in different TOUGH codes (e.g. EOS3 for enhanced geothermal system, ECO2N for CO_2 geological sequestration) is rebuilt to couple the phase equilibrium and geochemical reaction together.

2. Model Formulation and Mathematical Description

Mass Conservation Equations

The mathematical algorithm of reactive solute transport model is based on that of TOUGH2 (Pruess et al. 1999). TOUGH2 is a numerical simulator of multi-component, multiphase fluid and heat flow in porous media. In the TOUGH2 formulation, fluid advection is described with a multiphase extension of Darcy's law and there is diffusive mass transport in all phases. Heat flow occurs by conduction and convection, including sensible as well as latent heat effects. All the formulations are based on

the component mass and energy balance. The mass gain and loss from geochemical reactions are accounted by adding source/sink terms into the mass balance equation. The integral form of these balance equations is

$$\frac{\mathrm{d}}{\mathrm{d}t}\int_{V_n} M^{\kappa}\mathrm{d}V_n = \int_{\Gamma_n} \bar{F}^{\kappa}\cdot\hat{n}\mathrm{d}\Gamma_n + \int_{V_n} q^{\kappa}\mathrm{d}V_n + \int_{V_n} R^{\kappa}_{\mathrm{req}}\mathrm{d}V_n + \int_{V_n} R^{\kappa}_{\mathrm{r}}\mathrm{d}V_n \tag{1}$$

The integration is over an arbitrary sub-domain V_n of the flow system under study, which is bounded by the closed surface Γ_n. The quantity M appearing in the accumulation term represents mass of a primary components or species, with κ= 1, ..., NK, labeling the primary components or species (H_2O, CO_2, H^+, Ca^{2+}, ...). F denotes mass flux, and q denotes sinks and sources, n is a normal vector on surface element $\mathrm{d}\Gamma_n$, pointing inward into V_n. R_{req} represents mass generation and loss by the chemical equilibrium reaction. The total mass fraction of the primary components or species are tracked in the mass balance equations, so there is no necessity to compute the mass contributions from the aqueous equilibrium reactions, and only the mass generation or loss by the chemical equilibrium reactions between phases (aqueous and gas phases, aqueous and mineral phases) are taken into account in this sink or source term. The term of R_r is the sink or source generated by the kinetic chemical reactions.

$$M^{\kappa} = \phi\sum_{\beta} S_{\beta}\rho_{\beta}x^{\kappa}_{\beta} \tag{2}$$

The total mass of primary component or species κ is obtained by summing over the fluid phases β (= aqueous, gas, and NAPL). φ is porosity, S_β is the saturation of phase β (i.e., the fraction of pore volume occupied by phase β), ρ_β is the density of phase β, x^{κ}_{β} is the total mass fraction of primary component or chemical species κ present in phase β, and x^{κ}_{β} is the function of the concentration of related primary chemical species $c_{\mathrm{p},j}$, i.e., $x^{\kappa}_{\beta} = f(c_{\mathrm{p},j})$, the calculation details of X^{κ}_{β} will be discussed later.

The mass flux is advective mass flux and diffusive mass flux:

$$F^{\kappa} = F^{\kappa}_{\mathrm{adv}} + F^{\kappa}_{\mathrm{dis}} \tag{3}$$

Advective mass flux is a sum over phases,

$$F^{\kappa}_{\mathrm{adv}} = \sum_{\beta} x^{\kappa}_{\beta}F_{\beta} \tag{4}$$

The individual advective phase uxes are given by a multiphase version of Darcy's law:

$$F_{\beta} = \rho_{\beta}u_{\beta} = -k\left[\frac{k_{\mathrm{r}\beta}\rho_{\beta}}{\mu_{\beta}}\right]\left[\nabla P_{\beta} - \rho_{\beta}g\right] \tag{5}$$

where, u_β is the Darcy velocity (volume flux) in phase β, k is absolute permeability, $k_{\mathrm{r}\beta}$ is the relative permeability to phase β, μ_β is viscosity, and P_β is the fluid pressure in phase β, which is the sum of the pressure P of a reference phase (usually taken to be the gas phase), and the capillary pressure $P_{c\beta}$ (≤ 0). g is the vector of gravitational acceleration.

In addition to Darcy flow, mass transport can also occur by diffusion and hydrodynamic dispersion, as follows

$$F^{\kappa}_{\mathrm{dis}} = \sum_{\beta} \rho_{\beta}\bar{D}^{\kappa}_{\beta}\nabla x^{\kappa}_{\beta} \tag{6}$$

where, $\bar{D}^{\kappa}_{\beta}$ is the hydrodynamic dispersion tensor.

The diffusive flux of component κ in phase β is given by

$$F_{\text{dis}}^{\kappa} = -\phi\tau_0\tau_\beta\rho_\beta d_\beta^{\kappa}\nabla x_\beta^{\kappa} \tag{7}$$

where, d_β^{κ} is the molecular diffusion coefficient for component κ in phase β, $\tau_0\tau_\beta$ is the tortuosity which includes a porous medium dependent factor τ_0 and a coefficient τ_β that depends on phase saturation S_β, $\tau_\beta = \tau_\beta(S_\beta)$.

Energy Conservation Equations

The energy balance equation is derived by assuming that energy is a function of temperature only and energy flux in the porous media occurs by advection and heat conduction only.

$$\frac{\mathrm{d}}{\mathrm{d}t}\int_{V_n} U\,\mathrm{d}V_n = \int_{\Gamma_n} \bar{\bar{F}}\cdot\hat{n}\,\mathrm{d}\Gamma_n + \int_{V_n} q_{\mathrm{h}}\,\mathrm{d}V_n \tag{8}$$

The integration is over an arbitrary sub-domain V_n of the flow system under study, which is bounded by the closed surface Γ_n. U is the heat accumulation term of rock and fluid, F is the heat flux, and q_{h} is the heat sink and source by heat injection and withdraw.

The heat accumulation term in a multiphase system is as follows:

$$U = (1-\phi)\rho_R C_R T + \phi\sum_\beta S_\beta\rho_\beta h_\beta \tag{9}$$

where, ρ_{R} and C_{R} are, respectively, the grain density and the specific heat of the rock, T is the temperature, and h_β is the specific internal energy of phase β.

The heat flux is given by

$$F = -\lambda\nabla T + \sum_\beta h_\beta F_\beta \tag{10}$$

where, λ is the thermal conductivity, h_β is specific enthalpy in phase β, and F_β is given by Eq. 5.

Constraint Equations

There are four types of constraint equations in the fully coupled reative solute transport model, which includes:

Phase saturation

Sum of all phase saturations is equal to one.

$$\sum_{\beta=1}^{N_p} S_\beta = 1 \tag{11}$$

where, *Np* is the number of phases that are present in current reactive solute transport system.

Mass fraction

Sum of total mass fractions for all primary chemical species in phase β is equal to one.

$$\sum_{\kappa=1}^{N_c} x_\beta^{\kappa} = 1 \tag{12}$$

where, N_c is the number of primary chemical species or components selected in current reactive solute transport system.

Phase equilibrium

As the dissolution rates of gaseous phase in aqueous phase and aqueous phase in gaseous phase are very fast, the gaseous and aqueous phases are assumed to be in thermodynamic equilibrium. The equation for thermodynamics equilibrium is the equality of fugacities of the components in the gas and aqueous phases. We assume that the only water can be present in aqueous phase, and other chemical species in aqueous will not be present in the gaseous phase.

$$f_{g,\kappa} = f_{a,\kappa} \tag{13}$$

where, f is the fugacity of component κ. The number of thermodynamic equilibrium constraints is determined by the number of the equilibrium pairs that is present in the reactive solute transport model. The calculation details for the phase equilibrium will be discussed later.

Saturation index for gas and mineral at equilibrium condition

In a geochemical reaction system, the dissolution rate of a certain mineral (i.e., $CaCO_3$) is very fast. The reaction of the mineral is always set to be at equilibrium, the mineral saturation index controls the dissolution of the mineral, and it can be expressed as:

$$F_m = \log \Omega_m = \log \left[X_m^{-1} \lambda_m^{-1} K_m^{-1} \prod_{j=1}^{N_c} c_j^{v_{mj}} \gamma_j^{v_{mj}} \right] = 0 \tag{14}$$

where, m is the equilibrium mineral index, X_m is the mole fraction of the m-th mineral phase, λ_m is its thermodynamic activity coefficient (for pure mineral phases X_m and λ_m are taken equal to one), K_m is the corresponding equilibrium constant of the equilibrium mineral, C_j is the concentration of related primary chemical species or components, v_mj is the stoichiometric coefficient of j-th basis species in the m-th mineral equilibrium reaction, and j is the activity coefficient of primary chemical species.

According to the Mass-Action Law, one has:

$$F_g = \log \Omega_g = \log \left[\Gamma_g^{-1} p_g^{-1} K_g^{-1} \prod_{j=1}^{N_c} c_j^{v_{gj}} \gamma_j^{v_{gj}} \right] = 0 \tag{15}$$

where, subscript g is gas index, P is the partial pressure (in bar), Γ is the gas fugacity coefficient. For low pressures (in the range of atmospheric pressure), the gaseous phase is assumed to behave like an ideal mixture, and the fugacity coefficient is assumed to be one. At higher temperatures and pressures, such as boiling conditions in hydrothermal systems and CO_2 disposal in deep aquifers, the assumption of ideal gas and ideal mixing behavior is not valid, and the fugacity coefficients should be corrected according to temperatures and pressures (Spycher and Reed, 1988). For example, for the H_2O-CO_2 mixtures in boiling conditions, we assume that H_2O and CO_2 are real gases, but their mixing is ideal. v_{gj} is the stoichiometric coefficient of j-th basis species in the g-th gas equilibrium reaction, and j is the activity coefficient of primary chemical species.

Chemical Reaction Equations

Total mass fraction of primary chemical species

For representing a geochemical system, it is convenient to select a subset of N_C aqueous species as basis species (or component or primary species). All other species are called secondary species that include aqueous complexes, precipitated (mineral) and gaseous species. The number of secondary species must be equal to the number of independent reactions. Any of the secondary species can be represented as a linear combination of the set of basis species. Therefore, all the mass of the secondary species can be transfered to the mass of primary chemical species. The total concentration of primary species can be expressed as:

$$C_j = c_j + \sum_{k=1}^{N_x} v_{kj} c_k \qquad j = 1, \ldots, N_c \tag{16}$$

where, C and c are the total concentrations and individual concentrations (chemical reactions are always solved per kg of water, and concentration units used here are mol/kg which is close enough to mol/l when its density is close to 1 kg/l); subscripts j and k are the indices of basis species and aqueous complexes; N_C and N_x are the number of the primary and secondary species; v_{kj} is the stoichiometric coefficient of the basis species in the aqueous complexes.

The total mass fraction of the primary chemical species can be defined as:

$$x^{\kappa} = \frac{C^{\kappa} M^{\kappa}}{\rho_l} \qquad \kappa = 1, \ldots N_C \tag{17}$$

where, M^{κ} is the molecular weight of the primary chemical species, and ρ_l is the density of the aqueous phase.

Aqueous complex

The aqueous chemical reactions are assumed to be at local equilibrium. By making use of the mass action equation to the dissociation of the i-th aqueous complex, the concentrations of aqueous complexes can be expressed as functions of the concentrations of primary chemical species:

$$c_k = K_k^{-1} \gamma_k^{-1} \prod_{j=1}^{N_c} c_j^{v_{kj}} \gamma_j^{v_{kj}} \tag{18}$$

where, c_k is the molal concentration of k-th secondary aqueous complexation, and c_j is molal concentration of the j-th basis species, k and j are thermodynamic activity coefficients of secondary and primary species, and K_k is the equilibrium constant of the k-th secondary complexation reaction.

Kinetic mineral dissolution/precipitation

Kinetic rates could be functions of non-basis species as well. Usually the species appearing in rate laws happen to be basis species. In this model, we use a rate expression given by Lasaga et al. (1994):

$$r_n = f\left(c_1, c_2, \ldots, c_{N_c}\right) = \pm k_n A_n \left|1 - \Omega_n^{\theta}\right|^{\eta} \quad n = 1, \ldots, N_q \tag{19}$$

where, positive values of r_n indicate dissolution, and negative values precipitation, k_n is the rate constant (moles per unit mineral surface area and unit time) which is temperature dependent, A_n is the specific reactive surface area per kg H_2O, n is the kinetic mineral saturation ratio defined as in Eq. 14. N_q is the number of the mineral at kinetic conditions. The parameters θ and η must be determined from experiments; usually, but not always, they are taken equal to one. The temperature dependence of the reaction rate constant can be expressed reasonably well via an Arrhenius equation (Lasaga, 1984; Steefel and Lasaga, 1994). Since many rate constants are reported at 25°C, it is convenient to approximate rate constant dependency as a function of temperature, thus

$$k = k_{25} \exp\left[\frac{-E_a}{R}\left(\frac{1}{T} - \frac{1}{298.15}\right)\right] \tag{20}$$

Activity ceofficient of water, neutral aqueous species and charged aqueous species

Activity coefficients of charged aqueous species are computed by an extended Debye-Huckle equation and parameters derived by Helgeson et al. (1981).

Porosity change

Porosity changes in porous media are directly tied to volume changes as a result of mineral precipitation and dissolution. The molar volumes of minerals created by hydrolysis reactions (i.e., anhydrous phases, such as feldspars, reacting with aqueous fluids to form hydrous minerals such as zeolites or clays) are often larger than those of the primary reactant minerals; therefore,

constant molar dissolution-precipitation reactions may lead to porosity reductions. These changes are taken into account in the code as follows:

The porosity of the medium (fracture or matrix) is given by:

$$\phi = 1 - \sum_{m=1}^{N_m} fr_{\mathrm{m}} - fr_{\mathrm{u}} \tag{21}$$

where, nm is the number of minerals, fr_{m} is the volume fraction of mineral m in the rock ($V_{\mathrm{mineral}}/V_{\mathrm{medium}}$, including porosity), and fr_{u} is the volume fraction of non-reactive rock. As the fr_{m} of each mineral changes, the porosity is recalculated at each time step. The porosity is not allowed to go below zero.

Permeability change

The changes of rock permeability are calculated from changes in porosity using ratios of permeabilities calculated from the Carman-Kozeny relation (Bear, 1972), and ignoring changes in grain size, tortuosity and specific surface area as follows:

$$k = k_i \left(\frac{1-\phi_i}{1-\phi} \right)^2 \left(\frac{\phi}{\phi_i} \right) \tag{22}$$

where, k_{i} and ϕ_{i} are the initial permeability and porosity, respectively.

3. Numercial Method and Mathematical Description

Space Discretization

The mass balance equations (Eq. 1) are discretized in space using the integral finite difference method. Introducing appropriate volume averages, we have

$$\frac{\mathrm{d}M_n^\kappa}{\mathrm{d}t} = \frac{1}{V_n} \sum_m A_{nm} F_{nm}^\kappa + q_n^\kappa + R_{\mathrm{req},n} + R_{\mathrm{r},n} \tag{23}$$

where, M_n is the average value of M over V_n. Surface integrals are approximated as a discrete sum of averages over surface segments A_{nm}, F_{nm} denotes mass flux between two volume elements V_n and V_m, and q_n denotes sinks and sources by mass injection or withdraw at element n.

The discretization of advective flux can be expressed as:

$$F_{\beta,nm} = -k_{nm} \left[\frac{k_{\mathrm{r}\beta}\rho_\beta}{\mu_\beta} \right]_{nm} \left[\frac{P_{\beta,n} - P_{\beta,m}}{D_{nm}} - \rho_{\beta,nm} g_{nm} \right] \tag{24}$$

where, the subscripts ($_{nm}$) denote a suitable averaging at the interface between grid blocks n and m. $D_{nm} = D_n + D_m$ is the distance between the nodal points n and m, and g_{nm} is the component of gravitational acceleration in the direction from m to n.

The discretization of dffusive flux is given by

$$F_{\beta,\mathrm{dis},nm}^\kappa = -\sum_\beta \left[\phi \tau_0 \tau_\beta \rho_\beta d_\beta^\kappa \right]_{nm} \left[\frac{\left(x_\beta^\kappa\right)_m - \left(x_\beta^\kappa\right)_n}{D_{nm}} \right] \tag{25}$$

The energy balance equations (Eq. 6) are discretized in space using the integral finite difference method. Introducing appropriate volume averages, we have

$$\frac{\mathrm{d}U_n}{\mathrm{d}t} = \frac{1}{V_n}\sum_m A_{nm}F_{nm} + q_{\mathrm{h},n} \tag{26}$$

The discretization of heat ux is as follows:

$$F_{nm} = -\lambda_{nm}\left[\frac{T_n - T_m}{D_{nm}}\right] + \sum_\beta h_{\beta,nm}F_{\beta,nm} \tag{27}$$

Time Discretization and Solution Method

For the fully coupled approach, the mathematical equations for fluid flow, solute transport and geochemical reaction are solved simultaneously. Based on grid cell, the whole equation system for the multi-component reactive solute transport can be expressed as follows:

$$R_n^{\kappa,k+1} = M_n^{\kappa,k+1} - M_n^{\kappa,k} - \frac{\Delta t}{V_n}\left[\sum_m A_{nm}F_{nm}^{\kappa,k+1} + V_n q_n^{\kappa} + V_n R_{\mathrm{req},n}^{\kappa,k+1} + V_n R_{\mathrm{r},n}^{\kappa,k+1}\right] \tag{28}$$

$$F_m^{k+1} = F_m\left(c_{j,k+1}\right) \qquad j = 1,\ldots,N_c + N_p + N_g \tag{29}$$

$$F_g^{k+1} = F_g\left(c_{j,k+1}\right) \qquad j = 1,\ldots,N_c + N_p + N_g \tag{30}$$

For each volume element Vn, there are NEQ (N_C+N_p+N_g) equations, so that for a fully coupled reactive solute transport system with NEL grid blocks represents a total of $NEL\times NEQ$ coupled non-linear equations. The unknowns are the $NEL\times NEQ$ independent primary variables $\{c_j;\ j=1,\ \ldots,\ NEL\times NEQ\}$, which completely define the state of the reactive solute transport system at time level t^{k+1}. These equations are solved by Newton-Raphson iteration, which is implemented as follows. We introduce an iteration index p and expand the residuals R and F at iteration step p+1 in a Taylor series in terms of those at index p. The Taylor series expansion of residual equation for c_j (p is NR-iteration index):

$$R_n^{\kappa,k+1}\left(c_{j,p+1}\right) = R_n^{\kappa,k+1}\left(c_{j,p}\right) + \sum_{j=1}^{N_C+N_p+N_g}\left.\frac{\partial R_n^{\kappa,k+1}}{\partial c_j}\right|_p \left(c_{j,p+1} - c_{j,p}\right) = 0 \qquad \kappa = 1,\ldots,N_C \tag{31}$$

$$F_m^{k+1}\left(c_{j,p+1}\right) = F_m^{k+1}\left(c_{j,p}\right) + \sum_{j=1}^{N_C+N_p+N_g}\left.\frac{\partial F_m^{k+1}}{\partial c_j}\right|_p \left(c_{j,p+1} - c_{j,p}\right) \tag{32}$$

$$F_g^{k+1}\left(c_{j,p+1}\right) = F_g^{k+1}\left(c_{j,p}\right) + \sum_{j=1}^{N_C+N_p+N_g}\left.\frac{\partial F_g^{k+1}}{\partial c_j}\right|_p \left(c_{j,p+1} - c_{j,p}\right) \tag{33}$$

Retaining only terms up to first order, we obtain a set of $NEL\times NEQ$ linear equations for the increments ($c_{i,p+1}$-$c_{\mathrm{i,p}}$):

$$\sum_{j=1}^{N_C+N_p+N_g}\left.\frac{\partial R_n^{\kappa,k+1}}{\partial c_j}\right|_p \left(c_{j,p+1} - c_{j,p}\right) = -R_n^{\kappa,k+1}\left(c_{j,p}\right) \tag{34}$$

$$\sum_{j=1}^{N_C+N_p+N_g}\left.\frac{\partial F_m^{k+1}}{\partial c_j}\right|_p \left(c_{j,p+1} - c_{j,p}\right) = -F_m^{k+1}\left(c_{j,p}\right) \tag{35}$$

$$\sum_{j=1}^{N_C+N_p+N_g}\left.\frac{\partial F_g^{k+1}}{\partial c_j}\right|_p \left(c_{j,p+1} - c_{j,p}\right) = -F_g^{k+1}\left(c_{j,p}\right) \tag{36}$$

For the fully coupled approach, the fluid flow and reactive solute transport equations are solved simultaneously until the prescribed convergence criteria are satisfied. The transport equations are solved on a component-by-component basis, and the chemical equations are solved on a grid block by grid block basis at the same time.

Convergence Criteria

Refer to the Toughreact simulator (Xu et al., 2004), the convergence is achieved when the absolute value of the ratio between the relative increment of concentration and the concentration of primary components or species is less than a given convergence tolerance. The convergence criteria can be expressed as:

$$\frac{\left|\Delta c_{j,p+1}^{k+1}\right|}{c_{j,p}^{k+1}} \le \tau \qquad j = 1, 2, \cdots, N_c + N_p + N_g \tag{37}$$

where, τ is the convergence criterion, the default value is $\tau=10^{-4}$. As a consequence, although the iteration method becomes more robust, the rate of convergence may slow down in some cases. When a negative value of c_j is obtained, the corresponding mineral is considered exhausted and must be removed from the chemical system, and its corresponding equation disappears. In this case, the speciation in solution may change drastically. This might have a strong effect on kinetic rate laws. So when a change occurs in the mineral assemblage, one might have to limit the time step to retain accuracy in rate law integration. In addition, for a given time step the code checks that dissolution of a mineral cannot be greater than the amount present in the medium, in order to avoid over-dissolution.

4. Examples and Discussions

CO_2 geological sequestration is an effective solution to store CO_2 from burning of fossil fuels in geological formations. Saline aquifers have the largest capacity among the many options for long-term geological sequestration. They are large underground formations saturated with brine, and are often rich in dissolved minerals. CO_2 is injected into these aquifers as a supercritical fluid with a liquid-like density and a gas-like viscosity. The critical point of CO_2 (31.1 °C and 7.4 MPa) corresponds to an aquifer depth of about 800 m. It is believed that the mieral trapping (i.e. the mineral reaction between dissolved CO_2 and rock mineral) dominates the long-term fate after CO_2 sequestrated in geological formation. A better understanding of the geochemical reactions between CO_2 and dissolved minerals is important to evaluate the effectiveness of long-term CO_2 storage in geological formations. Here, we present two batch reaction systems with CO_2 geological sequestration to illustrate the fully coupled simulator in detail.

Phase Equilibrium Calculation

On the phase equilibrium calculation, the non-iterative approach (Spycher et al., 2003) of the original ECO2N module is preserved. The mutual solubilities of H_2O and CO_2 in the two coexisting phase is calculated by equating the chemical potentials. These solubilities are expressed by the mole fractions of CO_2 in liquid phase and H_2O in gas phase. The equilibrium of phases can be expressed by the relationship of equilibrium constant and fugacity:

$$\mathrm{H_2O(aq)} \rightleftharpoons \mathrm{H_2O(g)} \quad K_{\mathrm{H_2O}} = f_{\mathrm{H_2O(g)}} / a_{\mathrm{H_2O(aq)}} = \Phi_{\mathrm{H_2O(g)}} Y_{\mathrm{H_2O(g)}} P_{\mathrm{t}} / a_{\mathrm{H_2O(aq)}} \tag{38}$$

$$\mathrm{CO_2(g)} \rightleftharpoons \mathrm{CO_2(aq)} \quad K_{\mathrm{CO_2}} = f_{\mathrm{CO_2(g)}} / a_{\mathrm{CO_2(aq)}} = \Phi_{\mathrm{CO_2(g)}} Y_{\mathrm{CO_2(g)}} P_{\mathrm{t}} / a_{\mathrm{CO_2(aq)}} \tag{39}$$

where, K_i are equilibrium constants, f_i and Φ_i are the fugacity and fugacity coefficient of the gas components, a_i are the activities of components in the aqueous phase, Y_i is mole fraction of component i in the gas phase, and P_t is the total pressure.

The equilibrium constants for CO_2 and H_2O depend on temperature and pressure and such dependence can be described by an exponential function:

$$K_{(T,P)} = K^{0}_{(T,P^0)} \exp\left(\frac{\left(P - P^0\right)\bar{V}_i}{RT} \right) \tag{40}$$

where, V_i is the average partial molar volume of the pure condensed component i in the pressure range from P^0 to P, and P^0 is a reference pressure, here taken as 1 bar (and H_2O saturation pressure above 100°C).

In order to solve the mole fractions of H_2O and CO_2, some assumptions have been applied to the activities of H_2O and CO_2 (Spycher et al., 2003). The solubility of CO_2 in aqueous phase is relatively small at the pressure and temperature of interest. According to Raoult's law, the water activity (a_{H2O}) should be equal to its mole fraction in the aqueous phase. For a system where H_2O and CO_2 are the only two components, X_{H2O} is directly calculated as 1-X_{CO2}, such that

$$Y_{\mathrm{H_2O(g)}} = \frac{K^0_{\mathrm{H_2O}}\left(1 - X_{\mathrm{CO_2(aq)}}\right)}{\Phi_{\mathrm{H_2O(g)}}P_{\mathrm{t}}}\exp\left(\frac{\left(P - P^0\right)\bar{V}_{\mathrm{H_2O}}}{RT}\right) \tag{41}$$

Also, the relationship between activity of CO_2 and mole fraction of CO_2 shall be established to simplify Eqn.39. The activity coefficient can be accounted in the activity calculation of aqueous CO_2, i.e. $a_{CO2}=\gamma m_{CO2}$, in which γ is activity coefficient and m is molality of aqueous CO_2. For pure water, the activity coefficient is set to $\gamma=1/(1+m_{CO2}/55.508)$. The mole fraction of aqueous CO_2 can be computed by $X_{CO2}=m_{CO2}/(m_{CO2}+55.508)$. Then, we can derive that $a_{CO2}=55.508X_{CO2}$. These relationships yield

$$X_{\mathrm{CO_2(aq)}} = \frac{\Phi_{\mathrm{CO_2(g)}}\left(1 - Y_{\mathrm{H_2O(g)}}\right)P_{\mathrm{t}}}{55.508K^0_{\mathrm{CO_2(g)}}}\exp\left(-\frac{\left(P - P^0\right)\bar{V}_{\mathrm{CO_2}}}{RT}\right) \tag{42}$$

Eqns. 41 and 42 forms an equation system with two unknown variables (Y_{H2O} and X_{CO2}) and can be solved directly. If we define

$$A = \frac{K^0_{\mathrm{H_2O}}}{\Phi_{\mathrm{H_2O(g)}}P_{\mathrm{t}}}\exp\left(\frac{\left(P - P^0\right)\bar{V}_{\mathrm{H_2O}}}{RT}\right) \tag{43}$$

$$B = \frac{\Phi_{\mathrm{CO_2(g)}}P_{\mathrm{t}}}{55.508K^0_{\mathrm{CO_2(g)}}}\exp\left(-\frac{\left(P - P^0\right)\bar{V}_{\mathrm{H_2O}}}{RT}\right) \tag{44}$$

The solution to Eqns. 41 and 42 is

$$Y_{\mathrm{H_2O(g)}} = \frac{1 - B}{1/A - B} \tag{45}$$

$$X_{\mathrm{CO_2(aq)}} = B\left(1 - Y_{\mathrm{H_2O}}\right) \tag{46}$$

The above calculation is for the CO_2 solubility in pure water solution and H_2O solubility in CO_2 gaseous phase. In the modeled geochemical reaction system, there are several other chemical species in the aqueous phase, and the concentrations of these species will influence the solubility of CO_2 in the aqueous phase. The activity coefficient of aqueous CO_2 is therefore used to calibrate the solubility of CO_2 in saline water, the detail of which is given below.

The equation of activity coefficient for aqueous CO_2 in NaCl and other electrolyte solutions has been derived in many studies (Duan and Sun, 2003; Rumpf et al., 1994; He and Morse, 1993; Barta and Bradley, 1985; Nesbitt, 1984; Cramer, 1982; Drummond, 1981). The comparisons of these different methods (Spycher and Puress, 2004; Tsimpanogiannis et al., 2004) indicate that the correlation developed by Duan and Sun (2003) can reproduce the experimental solubilities accurately in a wide range of pressure. In our system, this correlation is used to calibrate the solubility of CO_2. The formulation of activity coefficient is a Pitzer formulation fitted to experimental solubility data, such that

$$\ln\left(\gamma^*\right) = 2\lambda\left(m_{\mathrm{Na}} + m_{\mathrm{k}} + 2m_{\mathrm{Ca}} + 2m_{\mathrm{Mg}}\right) + \xi m_{\mathrm{Cl}}\left(m_{\mathrm{Na}} + m_{\mathrm{K}} + m_{\mathrm{Ca}} + m_{\mathrm{Mg}}\right) - 0.07m_{\mathrm{SO_4}} \tag{47}$$

where, λ and ξ are functions of temperature T and pressure P, T is in Kelvin (273-533 K), P is in bar (0-2000 bar), m are molalities for aqueous species (for ionic strength ranging from 0 to 4.3 m, but up to 6 m NaCl and 4 m $CaCl_2$ in our P-T range of interest). Therefore, the solubility of CO_2 in electrolyte solutions can be calculated as follows:

$$\gamma^* = X^0_{CO2} / X_{CO2} \tag{48}$$

where, X^0_{CO2} is the aqueous CO_2 molality in pure water at P and T and X_{CO2} is the aqueous CO_2 molality in a saline solution with a composition defined by m_{Na}, m_K, m_{Ca}, m_{Mg}, m_{Cl} and m_{SO4} at the same P and T.

Batch reaction systerm of CO_2-NaCl-H_2O-$CaCO_3$

The batch reaction system includes saline water, CO_2 gas and solid calcite. Based on the most available geochemical and thermodynamic database such as EQ3/6 (Wolery, 1992), the potential geochemical reactions in the batch reaction system includes twelve aqueous chemical reactions, one calcite dissolution and one CO_2 gas dissolution. The chemical equations involved in the batch reaction system are listed in Tab.1. The aqueous chemical reactions, calcite dissolution and gas dissolution are set in equilibrium state in the batch reaction system. Two phases (aqueous and gaseous) are taken into account, i.e. the gaseous phase contains CO_2 and vaporized H_2O; the aqueous phase includes aqueous chemical species. These chemical reactions are controlled by the chemical equilibrium constants, which can be calculated from the EQ3/6 database (Wolery, 1992), and shown in Tab. 1. All the mathematical equations are developed based on the isothermal batch reaction model. The selected primary components or species are CO_2(g), H_2O, H^+, Na^+, Ca^{2+}, Cl^- and HCO_3^-. The equations for mass balance and chemical constraints in this batch reaction model are as follows:

$$\left[\varphi\rho_g S_g X_g^{CO_2}\right]' - \left[\varphi\rho_g S_g X_g^{CO_2}\right] + R^{CO_2} = 0 \tag{49}$$

$$\left[\varphi\left(\rho_g S_g x_g^{H_2O} + \rho_l S_l x_l^{H_2O}\right)\right]' - \left[\varphi\left(\rho_g S_g x_g^{H_2O} + \rho_l S_l x_l^{H_2O}\right)\right] + R^{H_2O} = 0 \tag{50}$$

$$\left[\varphi\rho_l S_l x_l^{H^+}\right]' - \left[\varphi\rho_l S_l x_l^{H^+}\right] + R^{H^+} = 0 \tag{51}$$

$$\left[\varphi\rho_l S_l x_l^{Na^+}\right]' - \left[\varphi\rho_l S_l x_l^{Na^+}\right] + R^{Na^+} = 0 \tag{52}$$

$$\left[\varphi\rho_l S_l x_l^{Ca^+}\right]' - \left[\varphi\rho_l S_l x_l^{Ca^+}\right] + R^{Ca^+} = 0 \tag{53}$$

$$\left[\varphi\rho_l S_l x_l^{Cl^-}\right]' - \left[\varphi\rho_l S_l x_l^{Cl^-}\right] - R^{Cl^-} = 0 \tag{54}$$

$$\left[\varphi\rho_l S_l x_l^{HCO_3^-}\right]' - \left[\varphi\rho_l S_l x_l^{HCO_3^-}\right] - R^{HCO_3^-} = 0 \tag{55}$$

$$F_{CaCO_3(s)} = \log\left[K^{-1}_{CaCO_3(s)} \frac{c_{Ca^{2+}}\gamma_{Ca^{2+}} c_{HCO_3^-}\gamma_{HCO_3^-}}{c_{H^+}\gamma_{H^+}}\right] = 0 \tag{56}$$

$$F_{CO_2(g)} = \log\left[\Gamma^{-1}_{CO_2(g)} P^{-1}_{CO_2(g)} K^{-1}_{CO_2(g)} \frac{c_{H^+}\gamma_{H^+} c_{HCO_3^-}\gamma_{HCO_3^-}}{c_{H_2O}\gamma_{H_2O}}\right] = 0 \tag{57}$$

Where, ' denotes after chemical equilibrium, R is the sink or source term from CO_2 gas dissolution and solid calcite dissolution, x is the mass fraction of primary species, C is the concentration of primary species, γ is the activity coefficients of chemical species, Γ is the fugacity coefficient of CO_2 gas, $P_{CO2(g)}$ is the partial pressure of CO_2 gas, and K is the equilibrium constants related to the chemical reactions.

The twelve aqueous complexes is defined as secondary species: OH^-, $CaCl^+$, $CaCl_2$(aq), CO_2(aq), CO_3^{2-}, NaCl(aq), $NaHCO_3$, $CaHCO_3^+$, $CaCO_3$(aq), $Ca(OH)^+$, NaOH(aq), and $NaCO_3^-$. The concentrations of the secondary species can be represented and calculated by the primary species. The algebraic relationships between the primary species and the secondary species are given in Tab. 1. Therefore, the total concentrations of the primary species can represent the compositions of the batch reaction system. The concentration can be transformed to the mass fraction of each species, and be input into the mass balance equation. The total concentration of the primary species can be expressed as follows:

$$C_{H_2O} = c_{H_2O} - K^{-1}_{CO_2(aq)}\gamma^{-1}_{CO_2(aq)}\left[\frac{c_{HCO_3^-}\gamma_{HCO_3^-}c_{H^+}\gamma_{H^+}}{c_{H_2O}\gamma_{H_2O}}\right] + K^{-1}_{OH^-}\gamma^{-1}_{OH^-}\left[\frac{c_{H_2O}\gamma_{H_2O}}{c_{H^+}\gamma_{H^+}}\right]$$
$$+K^{-1}_{CaOH^+}\gamma^{-1}_{CaOH^+}\left[\frac{c_{Ca^{2+}}\gamma_{Ca^{2+}}c_{H_2O}\gamma_{H_2O}}{c_{H^+}\gamma_{H^+}}\right] + K^{-1}_{NaOH^+}\gamma^{-1}_{NaOH^+}\left[\frac{c_{Na^+}\gamma_{Na^+}c_{H_2O}\gamma_{H_2O}}{c_{H^+}\gamma_{H^+}}\right] \quad (58)$$

$$C_{H^+} = c_{H^+} + K^{-1}_{CO_2}\gamma^{-1}_{CO_2}\left[\frac{c_{HCO_3^-}\gamma_{HCO_3^-}c_{H^+}\gamma_{H^+}}{c_{H_2O}\gamma_{H_2O}}\right] - K^{-1}_{CaOH^+}\gamma^{-1}_{CaOH^+}\left[\frac{c_{Ca^{2+}}\gamma_{Ca^{2+}}c_{H_2O}\gamma_{H_2O}}{c_{H^+}\gamma_{H^+}}\right]$$
$$-K^{-1}_{NaOH}\gamma^{-1}_{NaOH}\left[\frac{c_{Na^+}\gamma_{Na^+}c_{H_2O}\gamma_{H_2O}}{c_{H^+}\gamma_{H^+}}\right] - K^{-1}_{CaCO_3(aq)}\gamma^{-1}_{CaCO_3(aq)}\left[\frac{c_{Ca^{2+}}\gamma_{Ca^{2+}}c_{HCO_3^-}\gamma_{HCO_3^-}}{c_{H^+}\gamma_{H^+}}\right]$$
$$-K^{-1}_{CO_3^{2-}}\gamma^{-1}_{CO_3^{2-}}\left[\frac{c_{HCO_3^-}\gamma_{HCO_3^-}}{c_{H^+}\gamma_{H^+}}\right] - K^{-1}_{NaCO_3^-(aq)}\gamma^{-1}_{NaCO_3^-(aq)}\left[\frac{c_{Na^{2+}}\gamma_{Na^{2+}}c_{HCO_3^-}\gamma_{HCO_3^-}}{c_{H^+}\gamma_{H^+}}\right] - K^{-1}_{OH^-}\gamma^{-1}_{OH^-}\left[\frac{c_{H_2O}\gamma_{H_2O}}{c_{H^+}\gamma_{H^+}}\right] \quad (59)$$

$$C_{Ca^{2+}} = c_{Ca^{2+}} + K^{-1}_{CaOH^+}\gamma^{-1}_{CaOH^+}\left[\frac{c_{Ca^{2+}}\gamma_{Ca^{2+}}c_{H_2O}\gamma_{H_2O}}{c_{H^+}\gamma_{H^+}}\right] + K^{-1}_{CaCl^+}\gamma^{-1}_{CaCl^+}\left[\frac{c_{Ca^{2+}}\gamma_{Ca^{2+}}c_{Cl^-}\gamma_{Cl^-}}{1}\right]$$
$$-K^{-1}_{CaHCO_3^-}\gamma^{-1}_{CaHCO_3^-}\left[\frac{c_{HCO_3^-}\gamma_{HCO_3^-}c_{Ca^{2+}}\gamma_{Ca^{2+}}}{1}\right]K^{-1}_{CaCl_2}\gamma^{-1}_{CaCl_2}\left[\frac{c_{Ca^{2+}}\gamma_{Ca^{2+}}c^2_{Cl^-}\gamma^2_{Cl^-}}{1}\right]$$
$$+K^{-1}_{CaCO_3(aq)}\gamma^{-1}_{CaCO_3(aq)}\left[\frac{c_{Ca^{2+}}\gamma_{Ca^{2+}}c_{HCO_3^-}\gamma_{HCO_3^-}}{c_{H^+}\gamma_{H^+}}\right] \quad (60)$$

$$C_{HCO_3^-} = c_{HCO_3^-} + K^{-1}_{CO_2(aq)}\gamma^{-1}_{CO_2(aq)}\left[\frac{c_{HCO_3^-}\gamma_{HCO_3^-}c_{H^+}\gamma_{H^+}}{c_{H_2O}\gamma_{H_2O}}\right] - K^{-1}_{CO_3^{2-}}\gamma^{-1}_{CO_3^{2-}}\left[\frac{c_{HCO_3^-}\gamma_{HCO_3^-}}{c_{H^+}\gamma_{H^+}}\right]$$
$$-K^{-1}_{CaCO_3(aq)}\gamma^{-1}_{CaCO_3(aq)}\left[\frac{c_{Ca^{2+}}\gamma_{Ca^{2+}}c_{HCO_3^-}\gamma_{HCO_3^-}}{c_{H^+}\gamma_{H^+}}\right] + K^{-1}_{CaHCO_3(aq)}\gamma^{-1}_{CaHCO_3(aq)}\left[\frac{c_{Ca^{2+}}\gamma_{Ca^{2+}}c_{HCO_3^-}\gamma_{HCO_3^-}}{1}\right]$$
$$+K^{-1}_{NaCO_3^-(aq)}\gamma^{-1}_{NaCO_3^-(aq)}\left[\frac{c_{Na^{2+}}\gamma_{Na^{2+}}c_{HCO_3^-}\gamma_{HCO_3^-}}{c_{H^+}\gamma_{H^+}}\right] + K^{-1}_{NaHCO_3(aq)}\gamma^{-1}_{NaHCO_3(aq)}\left[\frac{c_{Na^{2+}}\gamma_{Na^{2+}}c_{HCO_3^-}\gamma_{HCO_3^-}}{1}\right] \quad (61)$$

$$C_{Na^+} = c_{Na^+} + K^{-1}_{NaCO_3^-(aq)}\gamma^{-1}_{NaCO_3^-(aq)}\left[\frac{c_{Na^{2+}}\gamma_{Na^{2+}}c_{HCO_3^-}\gamma_{HCO_3^-}}{c_{H^+}\gamma_{H^+}}\right] + K^{-1}_{NaCl}\gamma^{-1}_{NaCl}\left[\frac{c_{Na^+}\gamma_{Na^+}c_{Cl^-}\gamma_{Cl^-}}{1}\right]$$
$$+K^{-1}_{NaOH}\gamma^{-1}_{NaOH}\left[\frac{c_{Na^+}\gamma_{Na^+}c_{H_2O}\gamma_{H_2O}}{c_{H^+}\gamma_{H^+}}\right] + K^{-1}_{NaHCO_3(aq)}\gamma^{-1}_{NaHCO_3(aq)}\left[\frac{c_{Na^{2+}}\gamma_{Na^{2+}}c_{HCO_3^-}\gamma_{HCO_3^-}}{1}\right] \quad (62)$$

$$C_{Cl^-} = c_{Cl^-} + K^{-1}_{CaCl^+}\gamma^{-1}_{CaCl^+}\left[\frac{c_{Ca^{2+}}\gamma_{Ca^{2+}}c_{Cl^-}\gamma_{Cl^-}}{1}\right] + 2K^{-1}_{CaCl_2}\gamma^{-1}_{CaCl_2}\left[\frac{c_{Ca^{2+}}\gamma_{Ca^{2+}}c^2_{Cl^-}\gamma^2_{Cl^-}}{1}\right]$$
$$+K^{-1}_{NaCl}\gamma^{-1}_{NaCl}\left[\frac{c_{Na^+}\gamma_{Na^+}c_{Cl^-}\gamma_{Cl^-}}{1}\right] \quad (63)$$

The geochemical reactions between aqueous and mineral phases result in mass generation, i.e. CO_2 gas dissolution and calcite dissolution. The source or sink terms in the mass balance equation can be calculated from the dissolved concentration of calcite ($C_{CaCO3(s)}$) and the dissolved concentration of CO_2 ($C_{CO2(g)}$) . The algebraic relationships between them are shown by the chemical reaction equations in Tab. 1. The geochemical reaction between mineral and saline solution is dominated by equilibrium constant. The chemical reaction between CO_2 (g) and aqueous phase is CO_2 dissolution. It is set to be under equilibrium condition, and dominated by the partial pressure of CO_2 and the equilibrium constant. Therefore, nine governing equations (Eqns. 46-54) are solved by Newton-Raphson iteration. Nine primary variables are selected in the batch reaction model, i.e. C_{H2O}, C_{H+}, C_{Ca2+}, C_{Na+}, C_{HCO3-}, C_{Cl-}, $C_{CaCO3(s)}$, $C_{CO2(g)}$ and $P_{CO2(g)}$. The Jacobin matrix coefficients for the batch reaction model are given by

$$\begin{bmatrix} \times & \times & \times & \times & \times & & & \times & \\ \times & \times & \times & \times & \times & & \times & \times & \\ \times & \times & \times & & \times & \times & \times & & \\ \times & \times & & \times & \times & \times & & & \\ \times & \times & \times & \times & \times & & \times & \times & \\ & & \times & \times & & \times & & & \\ & \times & \times & & \times & & & & \\ & \times & & & \times & & & \times & \times \\ & & & & & & & \times & \times \end{bmatrix} \begin{bmatrix} \Delta c_{H_2O} \\ \Delta c_{H^+} \\ \Delta c_{Ca^{2+}} \\ \Delta c_{Na^+} \\ \Delta c_{HCO_3^-} \\ \Delta c_{Cl^-} \\ \Delta c_{CaCO_3(s)} \\ \Delta c_{CO_2(g)} \\ \Delta P_{CO_2(g)} \end{bmatrix} = \begin{bmatrix} R_{H_2O} \\ R_{H^+} \\ R_{Ca^{2+}} \\ R_{Na^+} \\ R_{HCO_3^-} \\ R_{Cl^-} \\ F_{CaCO_3(s)} \\ F_{CO_2(g)} \\ R_{CO_2(g)} \end{bmatrix} \tag{64}$$

The geochemical reaction system is in equilibrium, so the system reaches the equilibrium condition once CO_2 contacts with the aqueous phase. The initial input data for the batch reaction model are given in Tab. 2 and the initial concentrations of aqueous species are given in the first column of Tab. 3. The simulation result is given in Tab. 3. We can conclude that the two dissolution reactions of CO_2 gas and calcite dominate the batch reaction system. The concentrations of CO_2 (aq) and Ca^{2+} have a dramatic increase due to the dissolutions of CO_2 and calcite. TOUGHREACT simulator is also used to simulate the same batch reaction system; the validation with TOUGHREACT simulator is shown in Tab. 3. The maximum error is 5.25% of the dissolved concentration for CO_2 gas. The error may be resulted from the gas property calculated by real gas law in the fully coupled simulator, but the TOUGHREACT simulator uses the real gas law to calculate the property of CO_2 gas.

Batch reaction systerm of complex chemical kinetics

The fully coupled reactive solute transport model could be applied for both the equilibrium and kinetic minerals. The mineralogy used in this complex batch reaction system is similar to that commonly encountered in sedimentary basins. Apps (1996) presented a batch geochemical simulation of the evolution of Gulf Coast sediments as a basis for interpreting the chemical processes relating to the deep injection disposal of hazardous and industrial wastes. The initial mineral abundances used in the current batch reaction system, are refined from the geochemical modeling study by Xu et al. (2004a) and geochemical reaction modeling example in TOUGHREAT manual (Xu et al., 2004b). The initial mineral volume fraction and the distribution of the original mineral are shown in Fig. 4.

The specification of formation mineralogy is determined in part by the availability of data. Most studies related to the Tertiary Gulf Coast sediments are concentrated in the state of Texas. The principal reservoir-quality sandstones within that region are respectively, the Frio, the Vicksberg and the Wilcox formations, all of which are found within the lower Tertiary. Of the three formations, the Frio was chosen as a representative candidate for the sequestration of supercritical carbon dioxide. It is the shallowest of the three formations, but over much of its areal extent, it is located at depths between 5,000 and 20,000 ft, depths sufficient to ensure adequate CO_2 densities for effective storage.

Calcite was assumed to react with aqueous species at local equilibrium because its reaction rate is typically quite rapid. Dissolution and precipitation of other minerals are kinetically-controlled. Kinetic rates are a product of the rate constant and reactive surface area. Multiple mechanisms (including neutral, acid and base) are are used for the dissolution of minerals. Kinetic parameters: rate constant (k_{25}), the activation energy (E_a), and the power term (n) for each mechanism are listed in Tab. 4. At any pH the total rate is the sum of the rates via each mechanism.

In the batch reaction system, there are four kinds of geochemical reactions, i.e., aqueous equilibrium reactions, kinetic mineral dissolution and precipitation, equilibrium gas dissolution, and equilibrium mineral dissolution. Twelve chemical species are selected as primary species (H_2O, H^+, Ca^{2+}, Na^+, HCO_3^-, Cl^-, Mg^{2+}, K^+, Fe^{2+}, $SiO_2(aq)$, SO_4^{2-}, AlO_2^-). Thirty aqueous equilibrium chemical reactions form thirty secondary aqueous chemical species, which can be represented by the primary chemical species selected. Fourteen chemical reactions for kinetic mineral dissolution and precipitation are controlled by kinetic reaction rates. The primary chemical species, secondary chemical species, original rock minerals and sencondary rock chemicals are listed in Tab. 5.

From the simulation results, majority of the CO_2 gas is dissolved into aqueous phase after 3,680 years. During the dissolution of the acid CO_2 gas, the pH value continues to buffer from 4.6 to 7.6, which is shown in Fig. 6. Majority of the calcite are dissolved into aqueous phase, which is shown in Fig. 7. Among the original mineral compositions, the oligoclase has almost 50% volume fraction change, the Na-smectite and illite have minor precipitations, which is shown in Fig. 8. For the potential precipitated minerals, as shown in Fig. 9, significant ankerite and albite-low precipitate due to CO_2 injection and dissolution of alumino-silicate minerals. Minor smectite-Ca and very slight dawsonite precipitation occurs. No dolomite precipitation is observed in the simulation. The re-distribution of volume fractions for the rock minerals after 3,680 years' reaction with CO_2 is shown in Fig. 5.

Concluding Remarks

We have analyzed the conventional structure of the exsiting reactive solute transport simulators, i.e. sequential iteration approach. The TOUGHREACT simulator is taken as a representative code to illustrate the approach. On the basis of TOUGHREACT simulator, we have developed a general framework for the fully coupled reactive solute transport model, which can applied to diferent systems, e.g. CO_2 geological sequestration, CO_2/waterflooding/other EOR processes, and enhanced geothermal system. We presented the fundamental equations describing various gas-water-rock interactions in porous media, chemical equlibrium constraint equations relating chemical speciesconcentration, partial pressure, and temperature, and incorporated it alongside the mass and energy conservation equations of primary chemical components or species, which are already embedded in the TOUGH family code, the starting point for the fully coupled simulator. In addition, rock properties, namely permeability and porosity, are functions of the volume of potential dissolved and precipitated mineral that are obtained from the literature.

We verified the simulator formulation and numerical implementation using two batch reaction systems, i.e. a chemical equilibrium system (CO_2 (g)-H_2O-NaCl-$CaCO_3$), and complex geochemical reaction system with chemical equilibrium and kinetics. The detailed mathematical descriptions of the chemical equilibrium system were presented to illustrate the structure of the fully coupled model. We compared the results of the chemical equilibrium system to those from orginal TOUGHREACT simulator. We obtained a good match between the fully coupled reactive solute transport model and TOUGHREACT simulator. In addition, the second complex geochemical batch reaction system, considering the chemical equilibrium and kinetics simultaneously, is simulated to provide a better understanding of the chemical reaction in different systems.

Acknowledgements

This work was supported by the CMG Foundation and by the Assistant Secretary for Fossil Energy, Office of Coal and Power R&D through the National Energy Technology Laboratory under U.S. Department of Energy Contract Number DE-FC26-09FE0000988.

References

Ague, J. J., Brimhall, G. H., 1989. Geochemical modeling of steady state and chemical reaction during supergene enrichment of porphyry copper deposits. Economical Geology 84, 506-528.

Appelo, C.A.J., 1994. Cation and proton exchange, pH variations and carbonate reactions in a freshening aquifer. Water Resources Research 30 (10), 2793-2805.

Apps, J. A. 1996. An approach to modeling of the chemistry of waste fluid disposal in deep saline aquifers, In Apps, J. A., and Tsang, C. F. (eds.), Deep injection disposal of hazardous and industrial waste: Scientific and Engineering Aspects, p. 465-488, Academic Press, San Diego, California.

Barta, L., Bradley D.J. 1985, Extension of the specific interaction model to include gas solubilities in high temperatures brines. Geochimica Cosmochimica Acta 49, 195-203.

Bacona, D. H., Sassb, B. M., Bhargavab, M., Sminchakb, J., and Guptab, N. 2009. Reactive transport modeling of CO_2 and SO_2 injection into deep saline formations and their effect on the hydraulic properties of host rocks. Energy Procedia: 1, 3283-3290, 2009.

Bear, J. 1972. Dynamics of Fluids in Porous Media. American Elsevier Pub. Co.

Bethke, C. M. 2002. The GEOCHEMIST'S WORKBENCH version 4.0: a user's guide. Urbana, IL: University of Illinois.

Brimhall, G.H., Alpers, C.N., Cunnigham, A.B. 1985. Analysis of supergene ore-forming processes and ground water solute transport using mass balance principles. Economical Geology 80, 1227-1256.

Cederberg, G. A., Street, R., Leckie, J. O. 1985. A ground-water mass transport and equilibrium chemistry model for multicomponent systems. Water Resources Research 21 (8), 1095-1104.

Cramer, S. D. 1982. The solubility of methane, carbon dioxide, and oxygen in brines from 0 to 300°C. Report of Investigations 8706, U.S. Department of the Interior, Bureau of Mines.

Credoz, A., Bildstein, O., Jullien, M., Raynal, J., Pétronin, J. C., Lillo, M., Pozo, C., Geniaut, G. 2009. Experimental and modeling study of geochemical reactivity between clayey caprocks and CO_2 in geological storage conditions. Energy Procedia 1, 3445-3452.

Delshad, M., Pope, G. A., and Sepehrnoori, K. 1996. A Compositional Simulator for Modeling Surfactant Enhanced Aquifer Remediation, Journal of Contaminant Hydrology, 23, 303-327.

Drummond, S. E. 1981. Boiling and mixing of hydrothermal fluids: chemical effects on mineral precipitation. Ph.D. thesis, Pennsylvania State University, 1981.

Engesgaard, P., Kipp L, K. 1992. A geochemical transport model for redox-controlled movement of mineral fronts in groundwater flow systems: a case of nitrate removal by oxidation of pyrite. Water Resources Research 28 (10), 2829-2843.

Fathi Najafabadi, N., Han, C., Delshad, M., Sepehrnoori, K. 2009. Development of a Three Phase, Fully Implicit, Parallel Chemical Flood Simulator". SPE-119002. SPE Reservoir Simulation Symposium, 2-4 February 2009, The Woodlands, Texas, USA.

He, S., Morse, W. 1993. The carbonic acid system and calcite solubility in aqueous Na-K-Ca-Mg-Cl-SO_4 solutions from 0 to 90 °C. Geochimica Cosmochimica Acta 57, 3533-3554.

Helgeson, H. C., Kirkham, D. H., Flowers, D. C. 1981. Theoretical prediction of the thermodynamic behavior of aqueous electrolytes at high pressures and temperatures: IV. Calculation of activity coeffcients, osmotic coeffients, and apparent molal and standard and relative partial molal properties to 600 °C and 5 kb. Am. J. Sci., v. 281, p. 1249-1516.

Jacquemet, N., Pironon, J., and Saint-Marc, J. 2008. Mineralogical changes of a well cement in various HS-CO(-brine) fluids at high pressure and temperature. Environ. Sci. Technol. 42: 262-288.

Kaszuba, J. P., Janecky, D. R., Snow, M. G. 2005. Experimental evaluation of mixed fluid reactions between supercritical carbon dioxide and NaCl brine: relevance to the integrity of a geologic carbon repository. Chemical Geology 217, 277-29.

Lasaga, A. C., Soler, J. M., Ganor, J., Burch, T. E., Nagy, K. L. 1994. Chemical weathering rate laws and global geochemical cycles. Geochimica et Cosmochimica Acta, v. 58, p. 2361-2386.

Liu, C.W., Narasimhan, T.N., 1989. Redox-controlled multiple species reactive chemical transport. 1. Model development. Water Resources Research 25, 869-882.

Moridis, G. and Pruess, K. 1998. T2SOLV: An enhanced package of solvers for the TOUGH2 family of reservoir simulation codes, Geothermics, Vol. 27, No. 4, pp. 415-444.

Nesbitt, H. W. 1984. Calculation of the solubility of CO_2 in NaCl-rich hydrothermal solutions using regular solution equations. Chemical Geology 43, 319-330.

Nienhuis, P., Appelo, C.A.T., Willemsen, A., 1991. Program PHREEQM: Modified from PHREEQE for use in mixing cell flow tube. Free University, Amsterdam, The Netherlands.

Parkhurst, D.L., 1990. Ion association models and mean activity cofficients of various salts. In: Melchior, D.C., Bassett, R.L. (Eds.), Chemical Modeling in Aqueous Systems, ACS Symposium Series, 416. American Chemistry Society, Washington DC.

Parkhurst, D.L., Thorstenson, D.C., Plummer, L.N., 1980. PHREEQE: a computer program for geochemical calculations. US Geological Survey, Water Resources Investigation 80-96, 174 pp.

Parkhurst, D. L. and Appelo, C. A. J. 1999. User's guide to PHREEQC (V.2) - A computer program for speciation, batch-reaction, one-dimensional transport, and inverse geochemical calculations. US Geological Survey Water-Resources Investigations Report, US Department of the Interior, Denver, CO.

Simunek, J., Suares, D. L., 1994. Two-dimensional transport model for variably saturated porous media with major ion chemistry. Water Resources Research 30 (4), 1115-1133.

Regnault, Q., Lagneau, V., Catalctte, H., and Schneider, H. 2005. Experimental study of pure mineral phases/supercritical CO_2 reactivity: Implications for geological CO_2 sequestration. C. R. Geoscience. 337:1331-1339.

Regnault, O., Lagneau, V., Schneider, H. 2009. Experimental measurement of portlandite carbonation kinetics with supercritical CO_2. Chemical Geology, 265, 113-121.

Rumpf, B., Nicolaisen, H., Ocal, C., Maurer, G. 1994. Solubility of carbon dioxide in aqueous solutions of sodium chloride: experimental results and correlation. J. Solution Chem. 23, 431-448.

Spycher, N., Pruess, K., and Ennis-king, J. 2003. CO_2-H_2O mixtures in the geological sequestration of CO_2. I. Assessment and calculation of mutual solubilities from 12 to 100 °C and up to 600 bar. Geochimica et Cosmochimica Acta, Vol. 67, No. 16, pp. 3015-3031.

Spycher, N., and Pruess, K. 2004. CO_2-H_2O Mixtures in the geological sequestration of CO_2. II. Partitioning in chloride brines at 12-100 °C and up to 600 bars, Research Report, LBNL-56334, Lawrence Berkeley National Laboratory, Berkeley, CA.

Steefel, C. I., and Lasaga, A. C. 1994. A coupled model for transport of multiple chemical species and kinetic precipitation/dissolution reactions with applications to reactive flow in single phase hydrothermal system, Am. J. Sci., v. 294, p. 529-592.

Tsimpanogiannis, I. N., Pawar, R., Carey, J. W., and Lichtner, P. C. 2004. Review of the thermodynamic properties and their prediction using an equation of state for the system CO_2/H_2O/electrolyte mixtures. Hydrology, Geochemistry and Geology Group, EES-6, Los Alamos National Laboratory, Los Alamos, NM, 87545.

Walter, A. L., Frind, E. O., Blowes, D. W., Ptacek, C. J., Molson, J. W. 1994. Modeling of multicomponent reactive transport in groundwater. 2. Metal mobility in aquifers impacted by acidic mine tailings discharge. Water Resources Research 30 (11), 3149-3158.

Wei, L. 2012. Sequential Coupling of Geochemical Reactions With Reservoir Simulations for Waterflood and EOR Studies. SPE J. 17 (2): 469-484. SPE-138037-PA. http://dx.doi.org/10.2118/138037-PA.

White, S. P. 1995. Multiphase nonisothermal transport of systems of reacting chemicals. Water Resources Research 31, 1761-1772.

White, S. P., Allis, R. G., Moore, J., Chidsey, T., Morganb, C., Gwynn, W., Adams, M. 2005. Simulation of reactive transport of injected CO_2 on the Colorado Plateau, Utah, USA. Chemical Geology 217, 387-405.

Wigand, M., Carey, J. W., Schütt, H., Spangenberg, E., Erzinger, J. 2008. Geochemical effects of CO_2 sequestration in sandstones under simulated in situ conditions of deep saline aquifers. Applied Geochemistry, V. 23, I. 9, 2735-2745.

Wolery, T.J., 1992. EQ3/6, a software package for geochemical modeling of aqueous systems: package overview and installation guide (version 7.0). Lawrence Livermore Laboratory Report UCRL-MA-110662 PT I, livermore, CA, USA, 246 pp.

Xu, T., 1996. Modeling nonisothermal multicomponent reactive solute transport through variably saturated porous media. Ph.D. dissertation, University of La CorunÄ a, La CorunÄ a, Spain, 310 pp.

Xu, T., GeÂrard, F., Pruess, K., Brimhall, G., 1997. Modeling nonisothermal multiphase multispecies reactive chemical transport in geologic media. Lawrence Berkeley Laboratory Report LBL-40504, Berkeley, CA, USA, 79 pp.

Xu, T., Apps, J. A., and Pruess, K. 2003. Reactive geochemical transport simulation to study mineral trapping for CO2 disposal in deep arenaceous formations. Journal of Geophysical Research: Vol. 108, No. B2.

Xu, T., Apps, J. A., Pruess, K. 2004a. Numerical simulation of CO_2 disposal by mineral trapping in deep aquifers. Applied eochemistry: V. 19, 917-936.

Xu, T., Ontoy, Y., Molling, P., Spycher, N., Parini, M., and Pruess, K. 2004b. Reactive transport modeling of injection well scaling and acidizing at Tiwi Field Philippines, Geothermics, In press.

Xu, T., Sonnenthal, E., Spycher, N., and Pruess, K. 2004c. TOUGHREACT users guide: a simulation program for non-isothermal multiphase reactive geochemical transport in variably saturated geologic media. Earth Sciences Division, Lawrence Berkeley National Laboratory, University of California, Berkeley, CA.

Xu, T., Sonnenthal, E., Spycher, N., and Pruess, K. 2006. TOUGHREACT- A simulation program for non-isothermal multiphase reactive geochemical transport in variably saturated geologic media: applications to geothermal injectivity and CO2 geological sequestration. Comput. Geosci. 32,145-165.

Xu, T., Apps, J. A., Pruess, K., Yamamoto, H. . Injection of CO_2 with H_2S and SO_2 and subsequent mineral trapping in sandstone-shale formation. Lawrence Berkeley National Laboratory: Lawrence Berkeley National Laboratory. LBNL Paper LBNL-57426.

Xu, T., Apps, J. A., Pruess, K., Yamamoto, H. 2007. Numerical modeling of injection and mineral trapping of CO_2 with H_2S and SO_2 in a sandstone formation. Chemical Geology: 242, 319-346.

Xu T., Kharaka, Y. K., Doughty, C., Freifel, B. M., Daley, T. M. 2010. Reactive transport modeling to study changes in water chemistry induced by CO_2 injection at the Frio-I Brine Pilot, Chem. Geol.

Yeh, G. T., Tripathi, V. S. 1989. A critical evaluation of recent developments of hydrogeochemical transport models of reactive multichemical components. Water Resources Research 25 (1), 93-108.

Yeh, G. T., Tripathi, V. S., 1991. A model for simulating transport of reactive multispecies components: model development and demonstration. Water Resources Research 27 (12), 3075-3094.

Appendix I-Figures

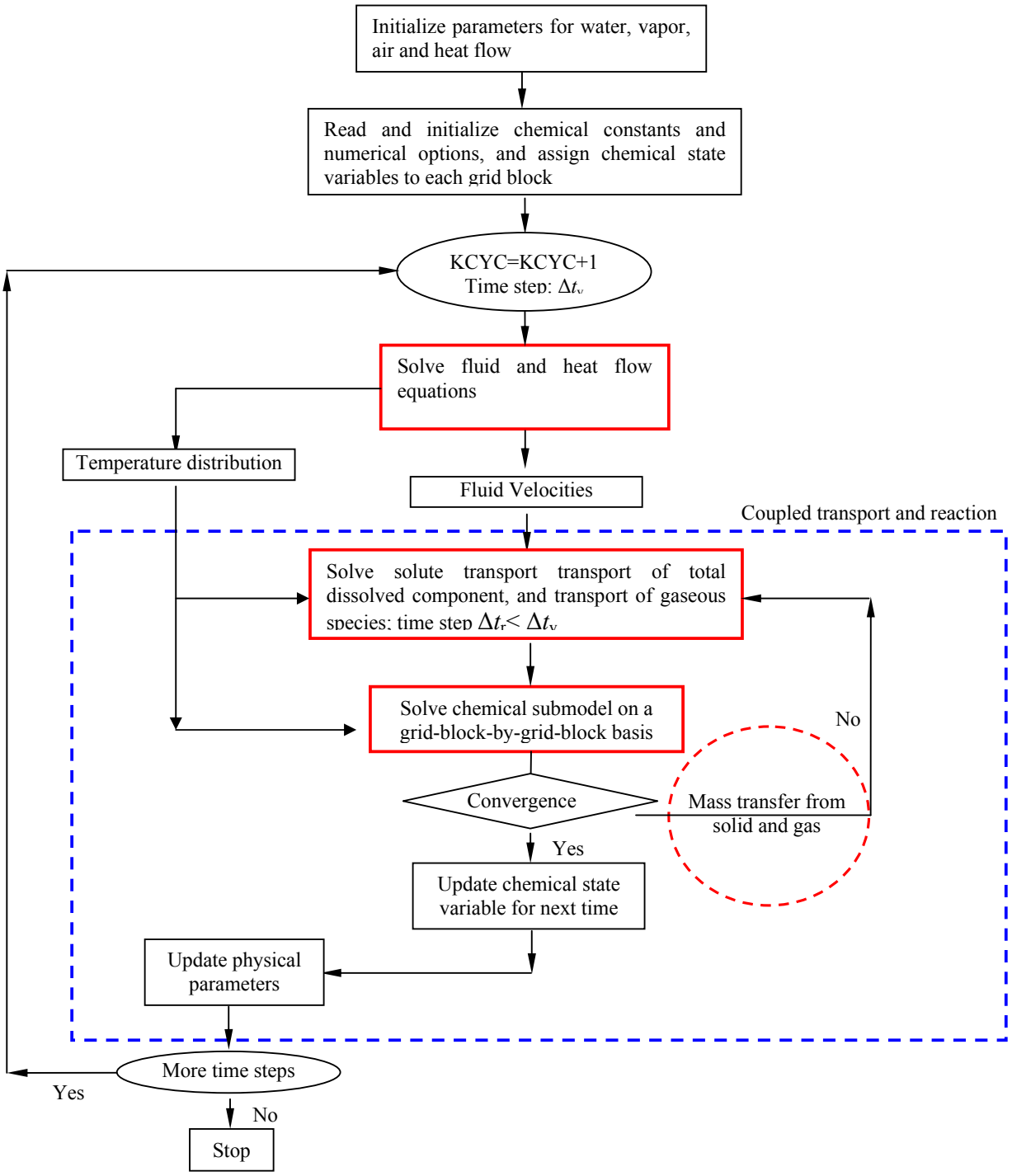

Figure 1 Flow chart of the TOUGHREACT simulator (Xu et al., 2004)

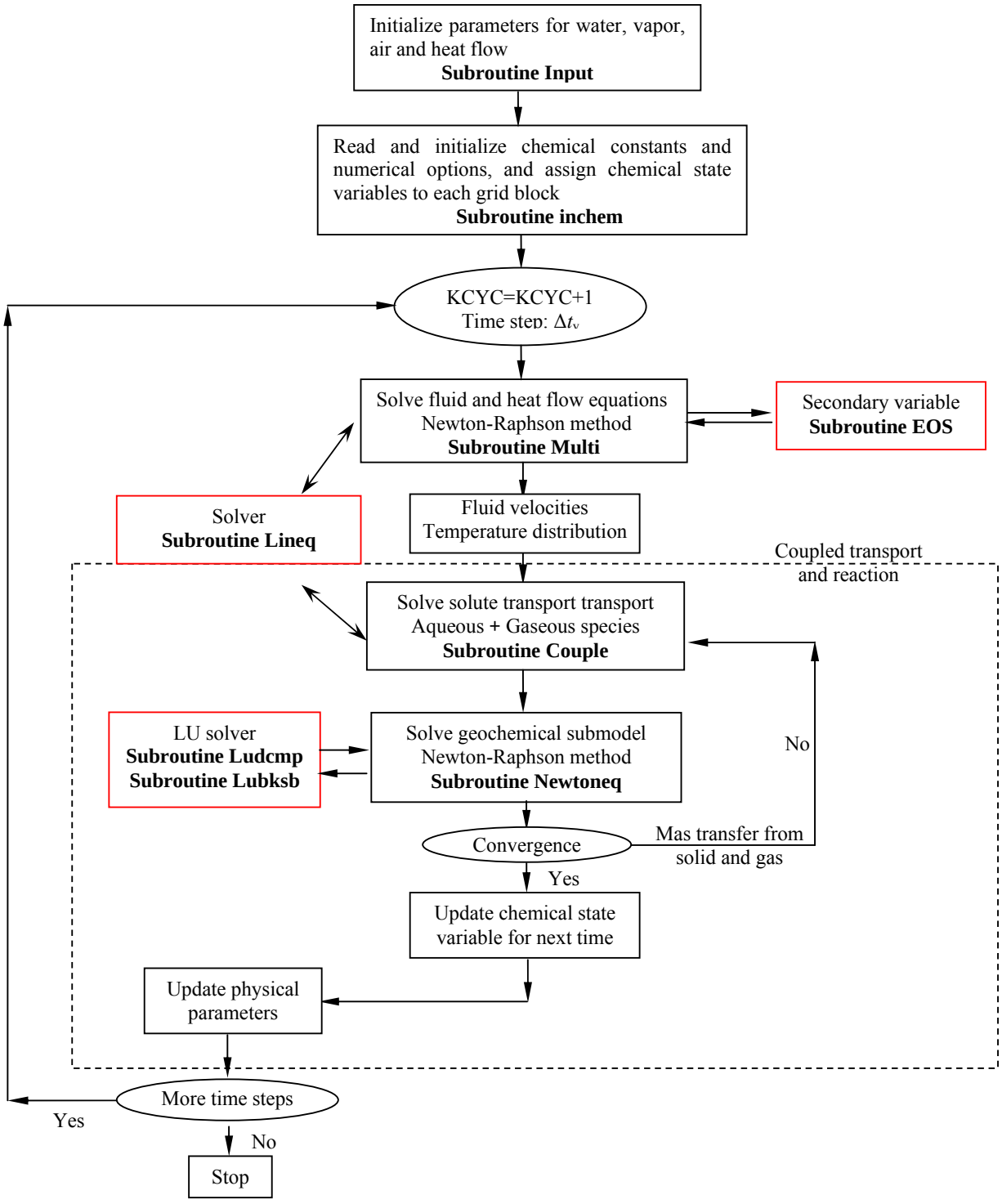

Figure 2 Code structure for the TOUGHREACT simulator

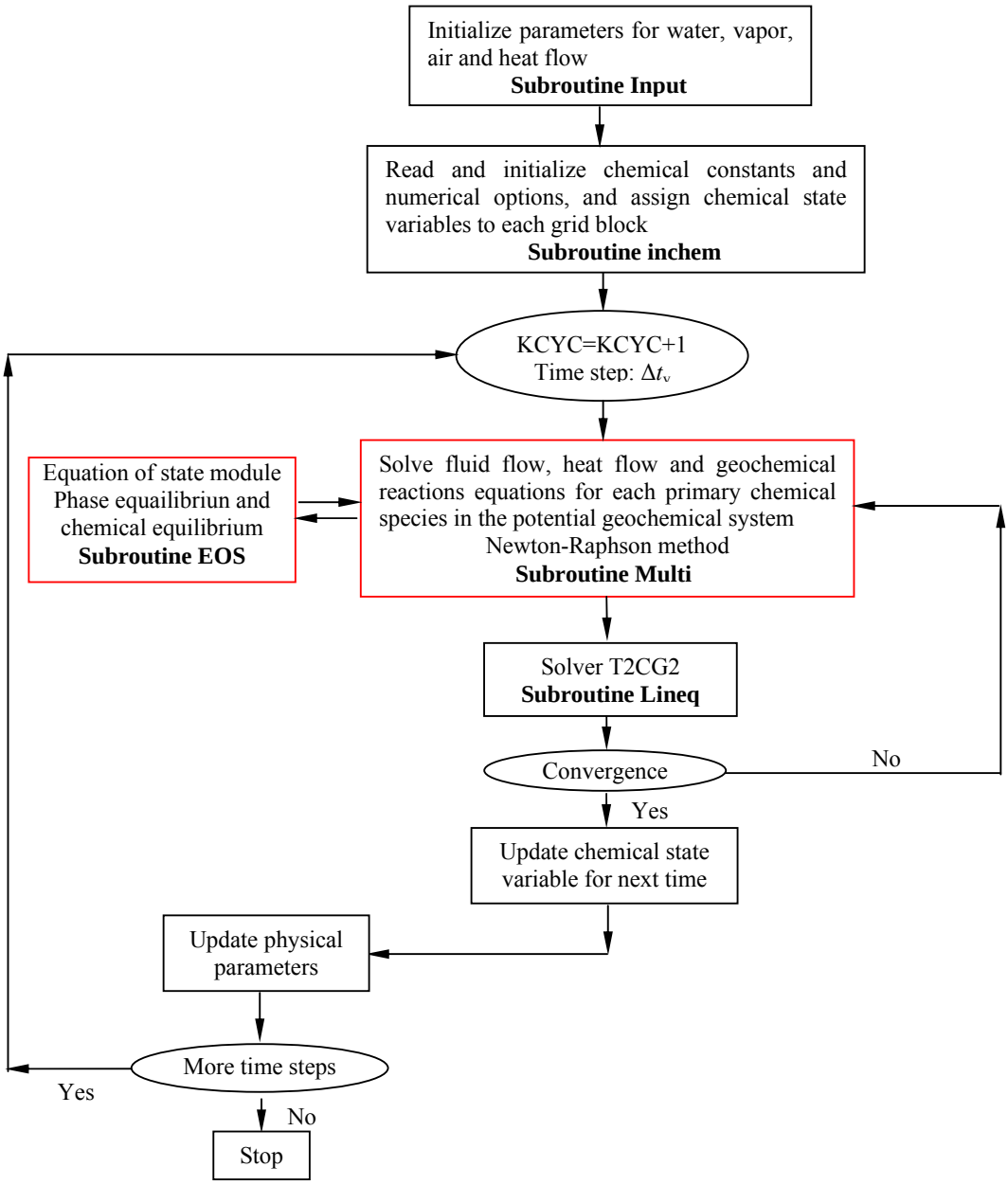

Figure 3 Code structure for the fully coupled reactive solute transport model

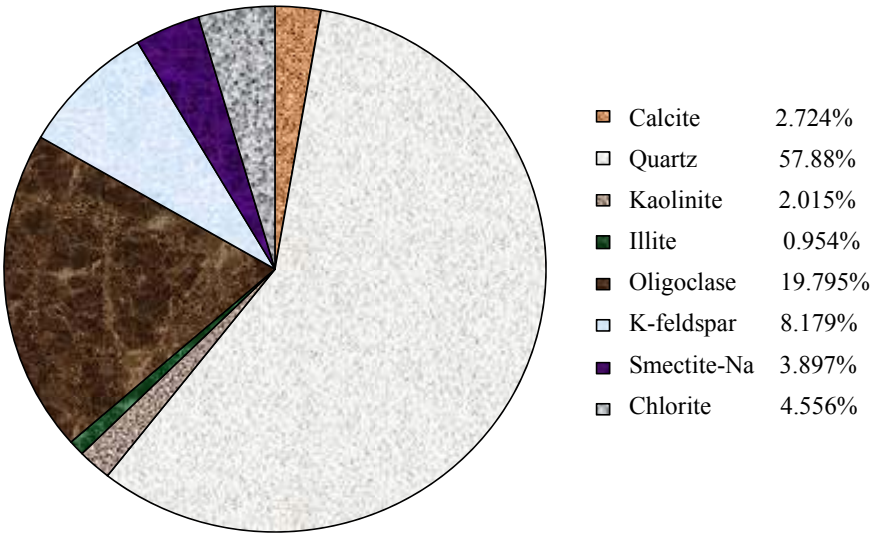

Figure 4 The original rock mineral compositions

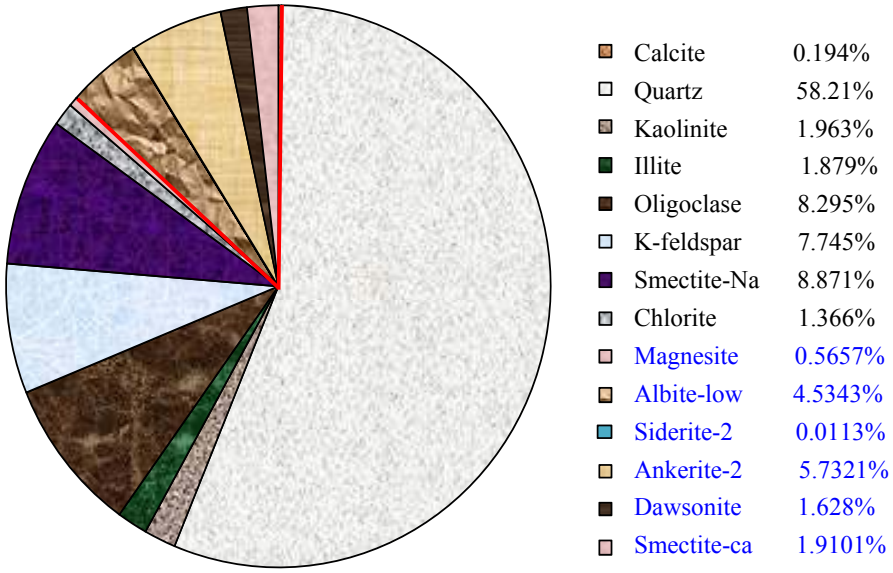

Figure 5 Mineral compositions after CO_2 squestration

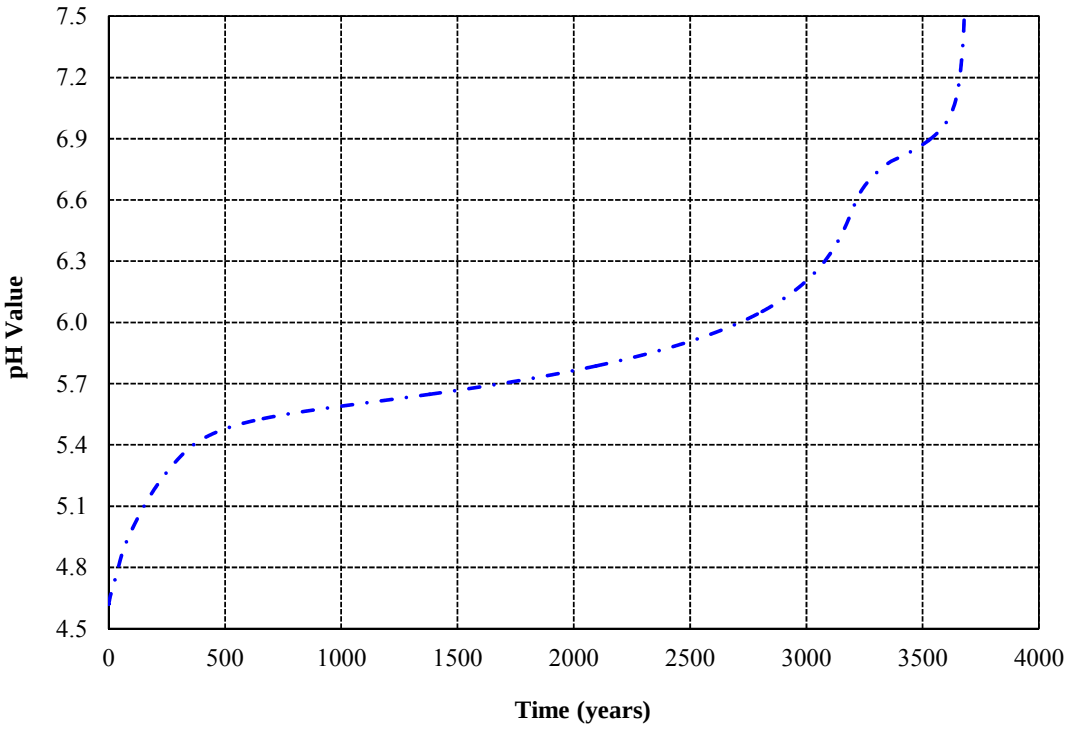

Figure 6 The evolution of pH value during CO_2 squestration

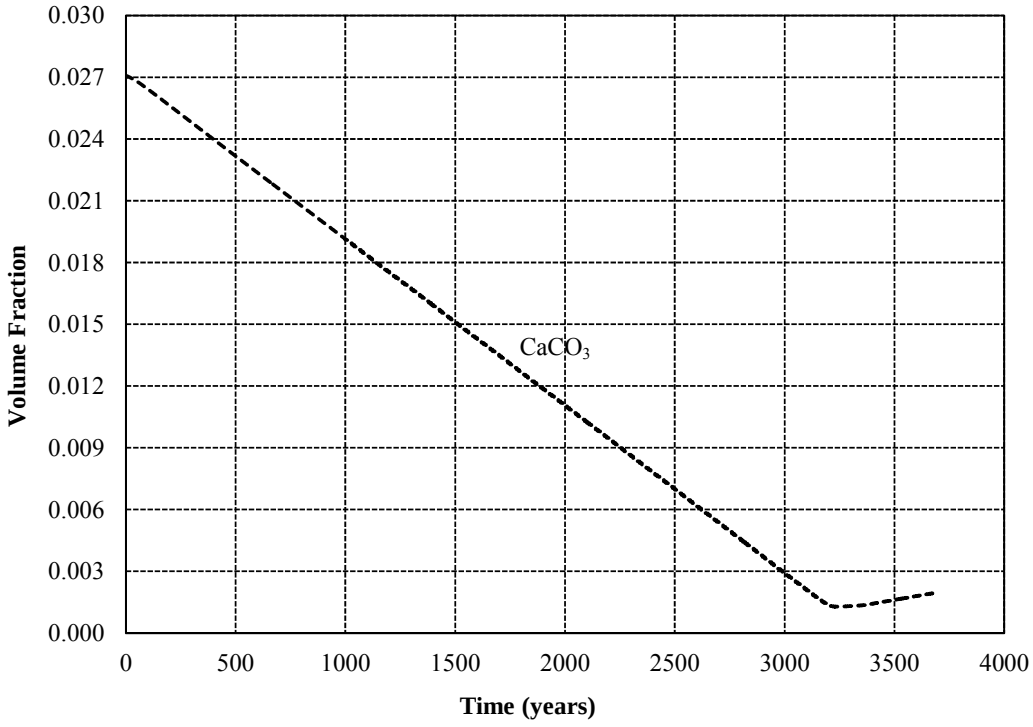

Figure 7 The volume fraction change of $CaCO_3$ in the rock matrix

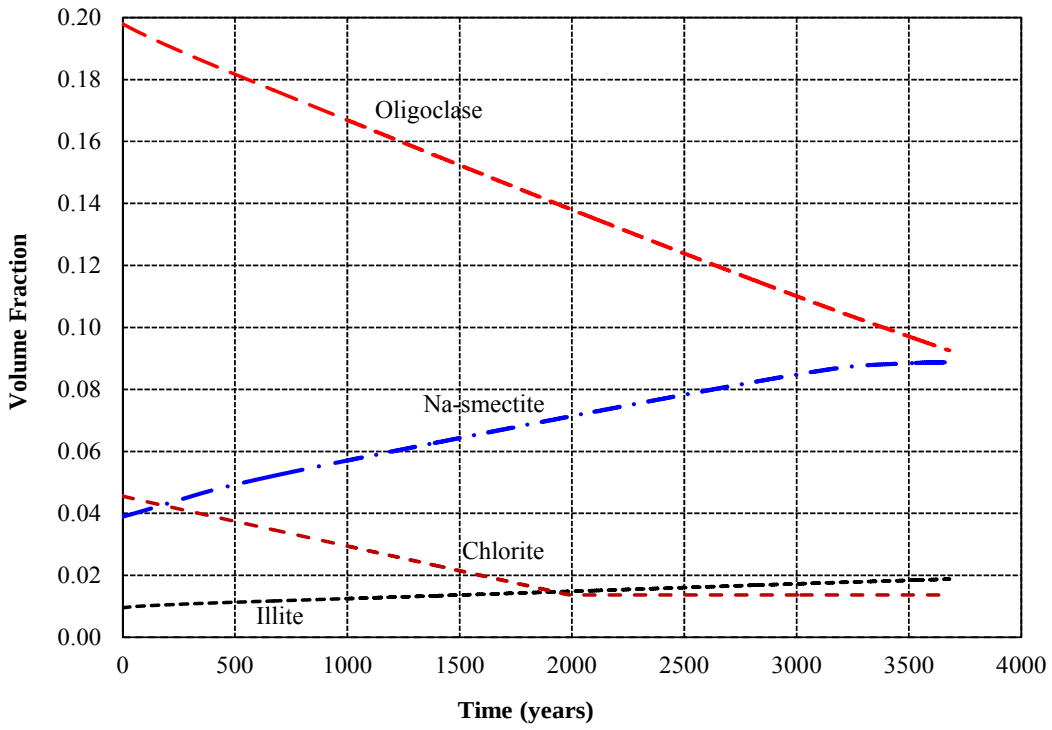

Figure 8 The volume fraction change of rock minerals in the rock matrix

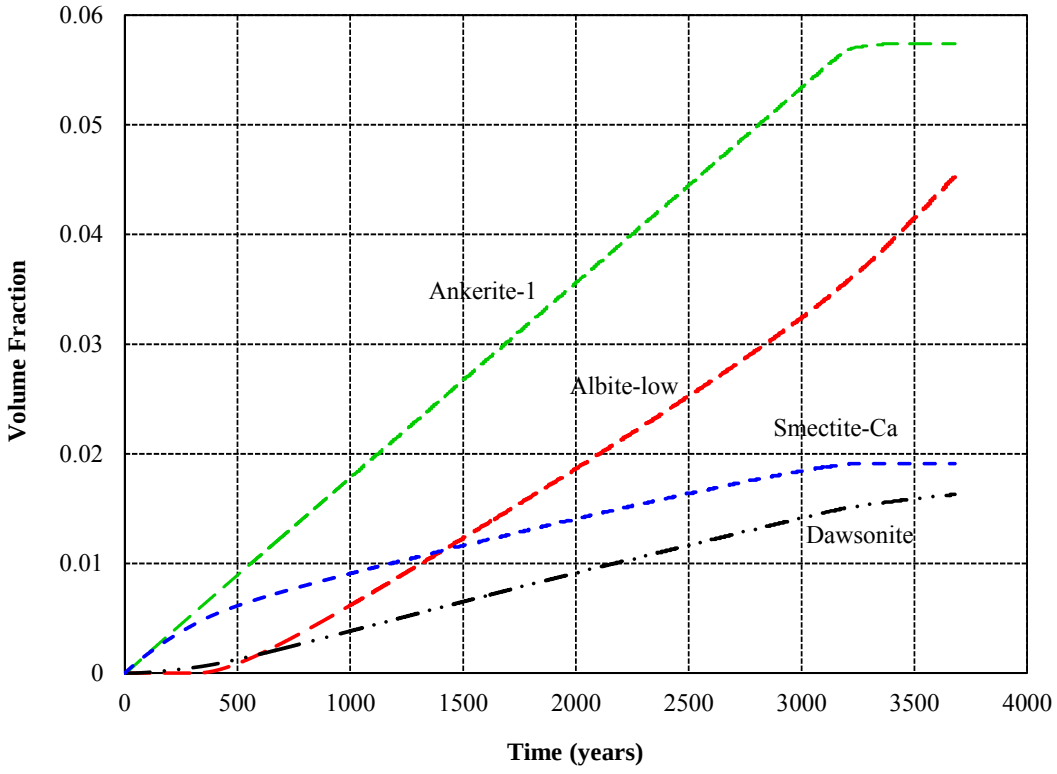

Figure 9 The volume fraction change of precipitated minerals in the rock matrix

Appendix II-Tables

Table 1 Equilibrium constants for chemical reactions in the batch system

Chemical Reactions	log *K*eq at 75 °C
$OH^- \rightleftharpoons H_2O - H^+$	12.70652234
$CaCl^+ \rightleftharpoons Ca^{2+} + Cl^-$	0.508190954
$CaCl_2(aq) \rightleftharpoons Ca^{2+} + 2Cl^-$	0.549797292
$NaCl(aq) \rightleftharpoons Na^+ + Cl^-$	0.582622874
$NaHCO_3(aq) \rightleftharpoons Na^+ + HCO_3^-$	0.23805711
$CaHCO_3^+ \rightleftharpoons Ca^{2+} + HCO_3^-$	-1.247810694
$CO_2(aq) \rightleftharpoons H^+ + HCO_3^- - H_2O$	-6.296079058
$CO_3^{2-} \rightleftharpoons HCO_3^- - H^+$	10.09857011
$CaCO_3(aq) \rightleftharpoons Ca^{2+} + HCO_3^- - H^+$	6.248545668
$Ca(OH)^+ \rightleftharpoons Ca^{2+} + H_2O - H^+$	11.21829089
$Na(OH)(aq) \rightleftharpoons Na + H_2O - H^+$	12.88172362
$NaCO_3^- \rightleftharpoons Na^+ + HCO_3^- - H^+$	10.26267908
Calcite mineral dissolution	
$CaCO_3(S) \rightleftharpoons Ca^{2+} + HCO_3^- - H^+$	1.114784395
Gaseous CO_2 dissolution	
$CO_2(g) \rightleftharpoons H^+ + HCO_3^- - H_2O$	-8.168289161

Table 2 Initial parameters of the batch reaction system

Parameter	Values
Gas Saturation (S_g)	0.5
Initial Pressure (P_i)	200 bar
Temperature (T)	75 °C
Porosity (φ)	0.3
Volume fraction of calcite	0.5
Volume fraction of non-reactive mineral	0.5

Table 3 Result comparison between the fully coupled simulator and TOUGHREACT

Species	Initial data	Fully-coupled Model	TOUGHREACT	Errors (%)
H_2O	1.0007777	1.0310173	1.0310335	0.0015778
H^+	3.0865518E-05	2.4055743E-05	2.3200153E-05	3.6878658
Ca^{2+}	4.4801997E-03	3.7897236E-02	3.7248307E-02	1.7421686
Na^+	0.9000024	0.8910427	0.8911388	0.0107810
HCO_3^-	1.9974637E-03	6.4692789E-02	6.3385779E-02	2.0619927
Cl^-	0.9106334	0.9125819	0.9124661	0.0126971
OH-	1.4343495E-08	1.8922409E-08	1.9503686E-08	2.9803428
$CaCl^+$	1.7247709E-04	1.3930015E-03	1.3709958E-03	1.6050865
$CaCl_2$(aq)	5.9203653E-05	4.6426897E-04	4.5762974E-04	1.4507863
NaCl(aq)	8.9297867E-02	8.6049929E-02	8.6185575E-02	0.1573874
$NaHCO_3$(aq)	4.2996252E-04	1.3361030E-02	1.3114010E-02	1.8836318
$CaHCO_3^+$	2.1416910E-05	5.5779795E-03	5.3798849E-03	3.6821350
CO_2(aq)	4.3136821E-02	1.0329780	0.9824600	5.1419873
CO_3^{2-}	3.7063587E-08	1.6250551E-06	1.6483202E-06	1.4114414
$CaCO_3$(aq)	2.1937727E-08	7.3491520E-06	7.3491650E-06	0.0001764
$CaOH^+$	2.7707266E-10	2.9609478E-09	3.0037454E-09	1.4248055
NaOH(aq)	3.6957495E-09	4.7122559E-09	4.8647524E-09	3.1347220
$NaCO_3^-$	3.1457201E-09	1.2977234E-07	1.3184608E-07	1.5728541
$CaCO_3$(s)	0.0	4.1862475E-02	4.0960340E-02	2.2024595
CO_2(g)	0.0	1.0623616	1.0093850	5.2483950
P_{co2}(bar)	197.71524	177.22620	168.49643	5.1809805

Note: The unit of the concentration of aqueous species is mol/l;
$CaCO_3$ concentration means dissolution concentration of solid $CaCO_3$ into aqueous phase;
CO_2 concentration means dissolution concentration of gaseous CO_2 into aqueous phase;
P_{CO2} is the partial pressure of gaseous CO_2.

Table 4 Kinetic parameters for mineral dissolution and precipitation(Xu et al., 2004)

Mineral	Surface area	Neutral mechanism		Acid mechanism			Base mechanism		
	(cm^2/g)	K_{25} ($mol/m^2 \cdot s$)	Ea(kJ/mol)	K_{25}	Ea	$n(H^+)$	K_{25}	Ea	$n(H^+)$
Quartz	9.8	1.023×10^{-14}	87.7	---	---	---	---	---	---
Kaolinite	151.6	6.918×10^{-14}	22.2	4.898×10^{-12}	65.9	0.777	8.913×10^{-18}	17.9	-0.472
Calcite	9.8	1.549×10^{-6}	23.5	5.012×10^{-1}	14.4	1	---	---	---
Illite	151.6	1.660×10^{-13}	35	1.047×10^{-11}	22.6	0.34	2.020×10^{-17}	58.9	-0.4
Oligoclase	9.8	1.445×10^{-12}	69.8	2.138×10^{-10}	65	0.457	---	---	---
K-feldspar	9.8	2.890×10^{-13}	38	8.710×10^{-11}	51.7	0.5	6.310×10^{-12}	94.1	-0.823
Na-smectite	151.6	1.660×10^{-13}	35	1.047×10^{-11}	22.6	0.34	2.020×10^{-17}	58.9	-0.4
Chlorite	9.8	2.020×10^{-13}	88	7.762×10^{-12}	88	0.5	---	---	---
Magnesite	9.8	4.571×10^{-10}	22.5	4.169×10^{-7}	14.4	1	---	---	---
Dolomite	9.8	2.951×10^{-8}	52.2	6.457×10^{-4}	36.1	0.5	---	---	---
Low-albite	9.8	2.754×10^{-13}	69.8	6.918×10^{-11}	65	0.457	2.512×10^{-16}	71	-0.572
Siderite	9.8	1.260×10^{-9}	62.76	6.457×10^{-4}	36.1	0.5	---	---	---
Ankerite	9.8	1.260×10^{-9}	62.76	6.457×10^{-4}	36.1	0.5	---	---	---
Dawsonite	9.8	1.260×10^{-9}	62.76	6.457×10^{-4}	36.1	0.5	---	---	---
Ca-smectite	151.6	1.660×10^{-13}	35	1.047×10^{-11}	22.6	0.34	2.020×10^{-17}	58.9	-0.4

Table 5 The chemical species and rock minerals present in the geochemical system

Primary sepcies and aqueous complex

H_2O	CO_2(aq)	$CaHCO_3^+$	$NaAlO_2$(aq)
H^+	CO_3^{2-}	$CaCO_3$(aq)	NaOH(aq)
Ca^{2+}	OH-	$CaOH^+$	$NaCO_3^-$
Mg^{2+}	$H_3SiO_4^-$	$FeCl^+$	NaCl(aq)
Na^+	Al^{3+}	$FeHCO_3^+$	$NaHCO_3$(aq)
K^+	$HAlO_2$(aq)	$FeCO_3$(aq)	$NaHSiO_3$(aq)
Fe^{2+}	$AlOH^{2+}$	$FeCl_4^{2-}$	$NaSO_4^-$
SiO_2(aq)	$Al(OH)_2^+$	KSO_4^-	
HCO_3^-	$Al(OH)_3$(aq)	KCl(aq)	
SO_4^{2-}	$CaCl^+$	$MgCl^+$	
AlO_2^-	$CaCl_2$(aq)	$MgSO_4$(aq)	
Cl^-	$CaSO_4$(aq)	$MgHCO_3^+$	

Primary minerals and their volume fractions

Calcite	$CaCO_3$	2.724%
Quartz	SiO_2	57.88%
Kaolinite	$Al_2Si_2O_5(OH)_4$	2.015%
Illite	$K_{0.6}Mg_{0.25}Al_{1.8}(Al_{0.5}Si_{3.5}O_{10})(OH)_2$	0.954%
Oligoclase	$CaNa_4Al_6Si_{14}O_{40}$	19.795%
K-feldspar	$KAlSi_3O_8$	8.179%
Smectite-Na	$Na_{0.29}Mg_{0.26}Al_{1.77}Si_{3.97}O_{10}(OH)_2$	3.897%
Chlorite	$Mg_{2.5}Fe_{2.5}Al_2Si_3O_{10}(OH)_8$	4.556%

Potential secondary minerals

Magnesite	$MgCO_3$
Albite-low	$NaAlSi_3O_8$
Dolomite	$CaMg(CO_3)_2$
Siderite	$FeCO_3$
Ca-smectite	$Ca_{0.145}Mg_{0.26}Al_{1.77}Si_{3.97}O_{10}(OH)_2$
Ankerite	$CaMg_{0.3}Fe_{0.7}(CO_3)_2$
Dawsonite	$NaAlCO_3\ (OH)_2$